

**KINETIC MODELLING OF SUCCINATE PRODUCTION
FROM GLUCOSE AND XYLOSE BY
ESCHERICHIA COLI KJ12201**



**A Thesis Submitted in Partial Fulfillment of the Requirements for the
Degree of Master of Science in Biotechnology
Suranaree University of Technology
Academic Year 2019**

การจำลองสมการจลนศาสตร์สำหรับการผลิตกรดซัลฟูริกจากกลูโคสและ
ไซโลส *ESCHERICHIA COLI* KJ12201



นายทัชศนนท์ ชาลิวงษ์

วิทยานิพนธ์นี้เป็นส่วนหนึ่งของการศึกษาตามหลักสูตรปริญญาวิทยาศาสตรมหาบัณฑิต
สาขาวิชาเทคโนโลยีชีวภาพ
มหาวิทยาลัยเทคโนโลยีสุรนารี
ปีการศึกษา 2562

**KINETIC MODELLING OF SUCCINATE PRODUCTION FROM
GLUCOSE AND XYLOSE BY *ESCHERICHIA COLI* KJ12201**

Suranaree University of Technology has approved this thesis submitted in partial fulfillment of the requirements for a Master's Degree.

Thesis Examining Committee



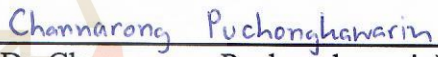
(Assoc. Prof. Dr. Apichat Boontawan)

Chairperson



(Assoc. Prof. Dr. Kaemwich Jantama)

Member (Thesis Advisor)



(Dr. Channarong Puchongkawarin)

Member



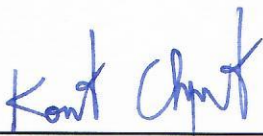
(Assoc. Prof. Dr. Chakkrit Umpuch)

Member



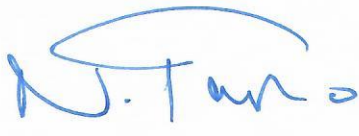
(Asst. Prof. Dr. Nawarat Nantapong)

Member



(Assoc. Prof. Ft. Lt. Dr. Kontorn Chamniprasart)

Vice Rector for Academic Affairs
and Internationalization



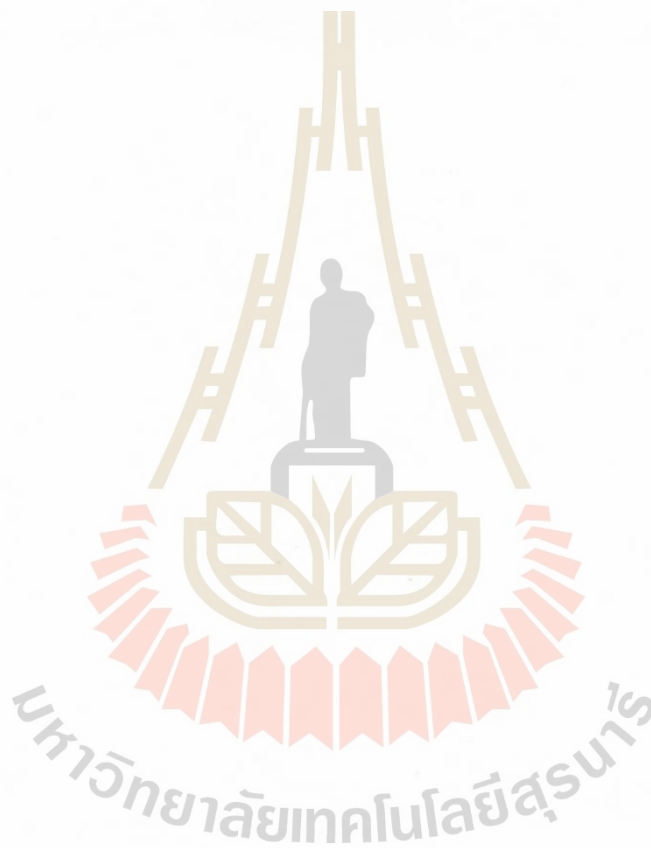
(Prof. Dr. Neung Teaumroong)

Dean of Institute of Agricultural
Technology

ทัชศนนท์ ชาลีวงษ์ : การจำลองสมการจลนศาสตร์สำหรับการผลิตกรดซัคซินิกจากกลูโคส และไซโลสด้วยเชื้อ *ESCHERICHIA COLI* KJ12201 (KINETIC MODELLING OF SUCCINATE PRODUCTION FROM GLUCOSE AND XYLOSE BY *ESCHERICHIA COLI* KJ12201) อาจารย์ที่ปรึกษา : รองศาสตราจารย์ ดร.เขมวิทช์ จันตะมา, 89 หน้า.

Escherichia coli KJ12201 เป็นหนึ่งในจุลินทรีย์ผู้ผลิตกรดซัคซินิกที่น่าสนใจ *E. coli* KJ12201 ได้ถูกปรับปรุงทางพันธุกรรมเพื่อพัฒนาประสิทธิภาพการผลิตกรดซัคซินิกจากไซโลส และกลูโคส ดังนั้นเพื่อทำการประเมินศักยภาพทางด้านของการเจริญของเซลล์ การบริโภคสารตั้งต้น และการผลิตกรดซัคซินิก *E. coli* KJ12201 จึงถูกเลี้ยงด้วยความเข้มข้นเริ่มต้นที่แตกต่างกันของไซโลสและกลูโคส จากการทดลองพบว่าอัตราการเจริญสูงสุดของ *E. coli* KJ12201 ในไซโลส สูงกว่าในกลูโคส อย่างไรก็ตามกรดซัคซินิกถูกผลิตสูงสุดที่ 0.835 ± 0.028 กรัมต่อกรัมของไซโลส และ 0.850 ± 0.013 กรัมต่อกรัมของกลูโคส ในขณะที่เดียวกันกรดอะซิติกถูกผลิตสูงสุดที่ 0.154 ± 0.031 กรัมต่อกรัมของไซโลส และ 0.108 ± 0.012 กรัมต่อกรัมของกลูโคส ยิ่งไปกว่านี้เพื่อทำการพัฒนาสมการจลนศาสตร์ การยับยั้งการเจริญของ *E. coli* KJ12201 จากความเข้มข้นของสารตั้งต้นและผลิตภัณฑ์ได้ถูกนำมาศึกษาและประเมิน สมการจลนศาสตร์ของ Haldane-Andrews, Monod, Aiba-Edward, และ Teissier ถูกนำมาใช้สำหรับการประมาณการยับยั้งที่เกิดจากสารตั้งต้น เมื่อพิจารณาการใช้ไซโลสเป็นสารตั้งต้นพบว่าที่ความเข้มข้นเริ่มต้นของไซโลสสูงกว่า 20 กรัมต่อลิตรยับยั้งการเจริญของ *E. coli* KJ12201 อย่างมีนัยสำคัญ ด้วยสมการจลนศาสตร์ของ Monod ซึ่งการทำนายมีความแม่นยำด้วยค่าความแปรปรวนที่ต่ำ ($\sigma^2 = 0.000342$) และค่าสัมประสิทธิ์การตัดสินใจที่สูง ($R^2 = 0.985$) แต่ในขณะที่เมื่อใช้กลูโคสเป็นสารตั้งต้นไม่พบการยับยั้งการเจริญของ *E. coli* KJ12201 และสมการจลนศาสตร์ของ Monod ได้ถูกนำมาใช้ในการทำนายค่าอัตราการเจริญของเชื้อได้อย่างแม่นยำด้วยค่าความแปรปรวนที่ต่ำ ($\sigma^2 = 0.000010$) และค่าสัมประสิทธิ์การตัดสินใจที่สูง ($R^2 = 0.998$) ในส่วนของการยับยั้งการเจริญด้วยกรดซัคซินิกจากการประมาณของสมการจลนศาสตร์ พบว่าความเข้มข้นที่เกิดการยับยั้งการเจริญของ *E. coli* KJ12201 ได้อย่างสมบูรณ์คือ 68.19 กรัมต่อลิตรและ 81.48 กรัมต่อลิตรสำหรับอาหารเลี้ยงเชื้อที่มีไซโลสและกลูโคสตามลำดับ แสดงให้เห็นว่า *E. coli* KJ12201 สามารถทนทานต่อการยับยั้งการเจริญที่ความเข้มข้นของกรดซัคซินิกสูงเมื่อใช้กลูโคสเป็นสารตั้งต้น เนื่องจาก ATP ที่ได้ถูกผลิตระหว่างกระบวนการไกลโคไลซิสจากการใช้กลูโคสเป็นสารตั้งต้นมีปริมาณมากกว่าจากการใช้ไซโลสเป็นสารตั้งต้น และถูกนำไปใช้เพื่อการเจริญและการดำรงอยู่ของเซลล์อย่างมีประสิทธิภาพมากกว่า ในท้ายที่สุดสมการจลนศาสตร์ได้ถูกพัฒนาเพื่อใช้ทำนายความเข้มข้นของเซลล์ การบริโภคของสารตั้งต้น การสร้างผลิตภัณฑ์ และการยับยั้งการเจริญจากสารตั้งต้นและผลิตภัณฑ์ตลอด

กระบวนการหมักที่ความเข้มข้นเริ่มต้นที่แตกต่างกันของไซโลสและกลูโคส ตัวแปรภายใน
สมการจลศาสตร์ได้ถูกคำนวณจากการลดความแตกต่างระหว่างผลการทดลองและผลลัพธ์จาก
การทำนายของสมการ หลังจากนั้นสมการจลศาสตร์ได้ถูกนำมาทดสอบยืนยันด้วยชุดข้อมูลอื่นๆ
จากการทดลอง ผลการทดลองแสดงให้เห็นว่าสมการจลศาสตร์สามารถทำนายตัวแปรได้
อย่างแม่นยำโดยสอดคล้องกับผลการทดลองจริง ดังนั้นผลลัพธ์จากการทดสอบชี้ให้เห็นว่า
สมการจลศาสตร์ที่ได้ถูกพัฒนาขึ้นสามารถนำมาใช้สำหรับการผลิตของกรดซักซินิก
จากไซโลสและกลูโคสอย่างมีประสิทธิภาพ



สาขาวิชาเทคโนโลยีชีวภาพ
ปีการศึกษา 2562

ลายมือชื่อนักศึกษา Jassanan Chaleenong
ลายมือชื่ออาจารย์ที่ปรึกษา U. Sambama
ลายมือชื่ออาจารย์ที่ปรึกษาร่วม Channarong Puchongkhamin

TASSANON CHALEEWONG : KINETIC MODELLING OF SUCCINATE
PRODUCTION FROM GLUCOSE AND XYLOSE BY *ESCHERICHIA COLI*
KJ12201. THESIS ADVISOR : ASSOC. PROF. KAEMWICH JANTAMA,
Ph.D., 89 PP.

KINETICS/MODELLING/SUCCINATE/*ESCHERICHIA COLI*

Escherichia coli KJ12201 is one of the promising succinate producers. *E. coli* KJ12201 was genetically modified to improve the succinate production proficiency from xylose and glucose. To evaluate its capability in the case of cell growth, substrate consumption, and succinate, *E. coli* KJ12201 was cultivated with various initial xylose and glucose concentrations. Based on the experimental data, the maximum specific growth rate of *E. coli* KJ12201 in xylose was greater than that of glucose. However, the maximum yield of succinate was 0.835 ± 0.028 g/g for xylose and 0.850 ± 0.013 g/g for glucose. Meanwhile, the maximum yield of acetate was 0.154 ± 0.031 g/g for xylose and 0.108 ± 0.012 g/g for glucose. Moreover, the substrate and succinate inhibition were elucidated and assessed for the kinetic model development. Substrate inhibition was examined in the substrate concentrations ranging from 20–80 g/L for xylose and glucose. Haldane-Andrews, Monod, Aiba-Edward, and Teissier models were used for predicting the substrate inhibition. Regarding xylose as a substrate, higher initial concentrations than 20 g/L significantly inhibited the cell growth rate. The Monod model appropriately predicted the xylose inhibition with the lowest variance ($\sigma^2 = 0.000342$) and an acceptable coefficient of determination ($R^2 = 0.985$). Meanwhile, glucose as a substrate had no inhibitory effect on the cell growth rate and the specific growth rate predicted using Monod model with low variance ($\sigma^2 = 0.000010$) and high

coefficient of determination ($R^2 = 0.998$). For succinate inhibition, the maximum succinate concentrations that completely inhibited the cell growth of *E. coli* KJ12201 were 68.19 g/L and 81.48 g/L in the medium containing xylose and glucose, respectively. These values demonstrated that *E. coli* KJ12201 could tolerate higher succinate concentration in glucose as a substrate than that of xylose since ATP produced from glucose during glycolysis was more than that of xylose and could more efficiently distribute to cell growth and cell maintenance. Finally, the kinetic model was developed to predict the cell concentration, substrate utilization, product formation, and inhibitory effects of substrate and product throughout the fermentation process at various initial xylose and glucose concentrations. The kinetic parameters of the proposed model were determined by minimizing the gap between experimental data and model prediction. Then, the proposed model was validated with another set of experimental data. The results showed that the proposed model precisely predicted kinetic parameters that suited well with experimental measurements. This indicated that the proposed model can be employed for efficiently predicting the succinate production from glucose and xylose.

School of Biotechnology

Academic Year 2019

Student's Signature Jassanon Chalceony

Advisor's Signature N. Santama

Co-Advisor's Signature Chanmarong Puchonghanarin

ACKNOWLEDGEMENTS

I would like to express my deep gratitude to Assoc. Prof. Dr. Kaemwich Jantama, my advisor, for his support, guidance, enthusiastic encouragement, and useful recommendations of this research work. I would also like to thank Dr. Channarong Puchongkawarin, my co-adviser, for his great advice and assistance in applying and troubleshooting the mathematic model on this project. My grateful thanks are also extended to Dr. Panwana Khunnonkwao who constructed *E. coli* KJ12201 used in this study, and Suraneree University of Technology (SUT) for supporting a fully academic fund under One Research One Graduation Scholarship (OROG).

Finally, I would also like to extend my thanks to all members in faculty of metabolic and bioprocess engineering in the School of Biotechnology in SUT, Nonthaporn Wong, Pachamon Pichayajittipong, Weeranat Sukullikkharesima, Sokra In, Chutchawan Phosiran, Sokha Kory, Saiparn Wannasiriwattana, and Kanyarat Onsanoi for their help in my research work.

Tassanon Chaleewong

CONTENTS

	Page
ABSTRACT IN THAI	I
ABSTRACT IN ENGLISH	III
ACKNOWLEDGEMENTS	V
CONTENTS	VI
LIST OF TABLES	IX
LIST OF FIGURES	XI
LIST OF ABBREVIATIONS	XIV
CHAPTER	
I INTRODUCTION	1
1.1 Rationale of the study	1
1.2 Research objectives	4
1.3 Scope and limitations	4
II REVIEW OF THE LITERATURE	5
2.1 Succinate applications and its production	5
2.2 Succinate fermentation	8
2.3 Batch fermentation kinetics	20
2.4 Fundamental unstructured growth kinetic model	22
2.5 Kinetics for substrate and product inhibition	25
2.6 Rates of substrate consumption and product formation	29

CONTENTS (Continued)

		Page
III	MAT ERIALS AND METHODS	31
	3.1 Microbial strains and inoculum preparation.....	31
	3.2 Fermentation process and conditions.....	32
	3.2.1 Effect of substrate concentration.....	32
	3.2.2 Effect of product concentration.....	32
	3.3 Biomass and metabolites analysis.....	33
	3.4 Fermentation parameter calculation.....	33
	3.5 Kinetic model development.....	34
	3.6 The estimation of kinetic parameters.....	37
	3.6.1 Sensitivity analysis.....	37
	3.6.2 Model calibration.....	38
	3.6.3 Model validation.....	38
IV	RESULTS AND DISCUSSION	40
	4.1 Fermentation profiles with single substrate.....	40
	4.1.1 <i>E. coli</i> KJ12201 growth.....	40
	4.1.2 Substrate consumption.....	42
	4.1.3 Product formation.....	43
	4.2 The effect of succinate inhibition.....	48
	4.3 Model development.....	50
	4.3.1 The specific growth rate model.....	50
	4.3.2 Sensitivity analysis.....	56

CONTENTS (Continued)

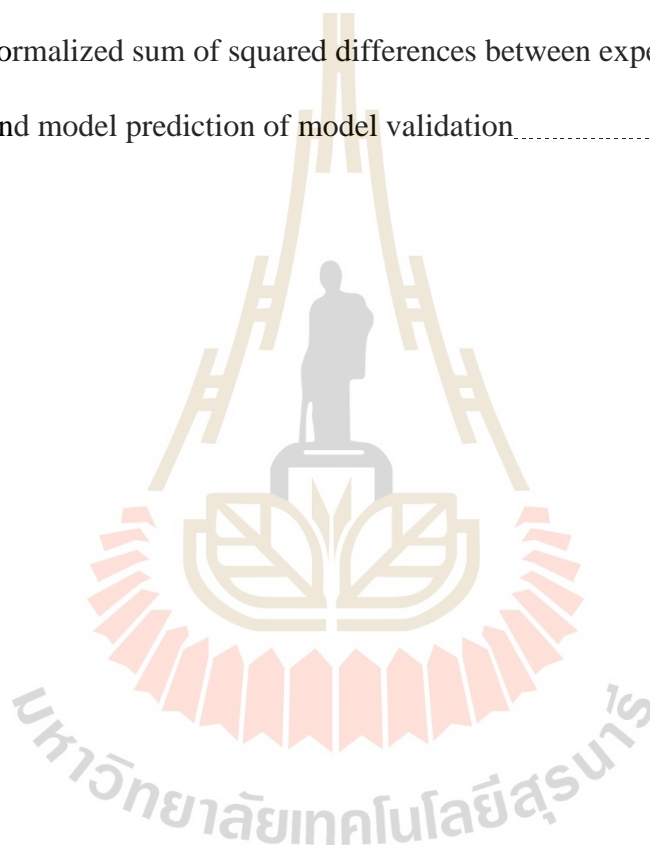
	Page
4.3.3 Model calibration.....	61
4.3.4 Model validation.....	66
V SUMMARY AND FUTURE PLAN.....	68
5.1 Summary.....	68
5.2 Future plan.....	69
REFERENCES.....	70
APPENDICES.....	79
BIOGRAPHY.....	88

LIST OF TABLES

Table	Page
2.1 Physical and chemical properties of succinate.....	6
2.2 Succinate production by <i>A. succinogenes</i>	11
2.3 Succinate production by <i>C. glutamicum</i>	12
2.4 Succinate production by <i>E. coli</i>	13
2.5 Succinate production by <i>M. succiniciproducens</i>	14
2.6 Succinate production by <i>S. cerevisiae</i>	14
4.1 The summary of fermentation parameters with single substrate.....	47
4.2 Estimated parameters and statistic measures obtained from various models.....	53
4.3 The parameters of specific growth rate model of each succinate producer.....	55
4.4 The relative and absolute parametric sensitivity for model prediction of xylose.....	59
4.5 The relative and absolute parametric sensitivity for model prediction of glucose.....	60
4.6 Estimated values of parameters for the fermentation process by <i>E. coli</i> KJ12201 with various initial concentrations of xylose and glucose.....	62

LIST OF TABLES (Continued)

Table		Page
4.7	The normalized sum of squared differences between experimental data and model prediction of model calibration.....	64
4.8	The normalized sum of squared differences between experimental data and model prediction of model validation.....	67



LIST OF FIGURES

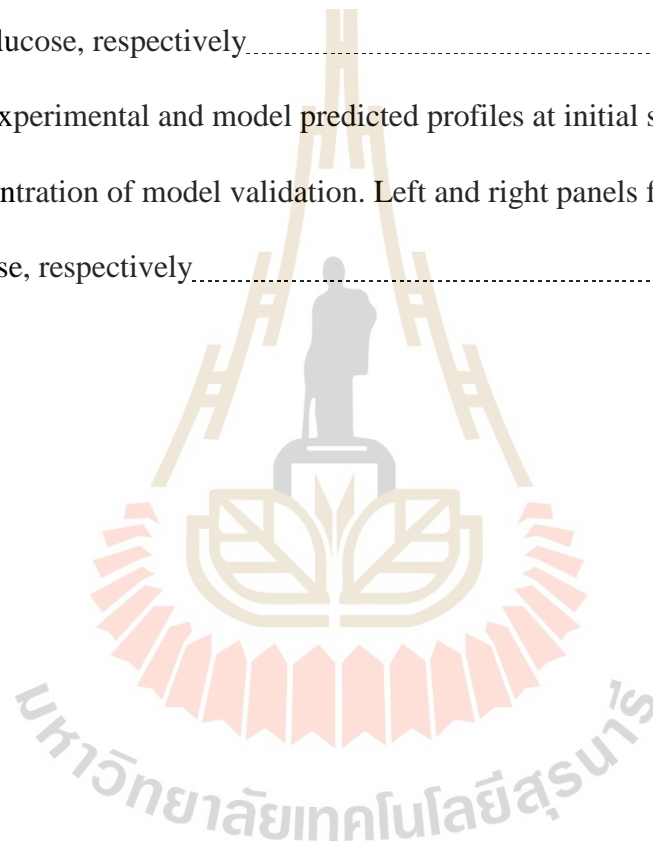
Figure	Page
2.1 The twelve sugar-based building blocks.....	6
2.2 Chemicals and products derived from succinate.....	7
2.3 The increase of worldwide succinate production.....	8
2.4 Succinic acid production pathways in microorganism.....	9
2.5 Construction steps of strain KJ122 from the parental <i>E. coli</i> C.....	15
2.6 Genes deletion of <i>E. coli</i> strain KJ073 to design KJ122 for producing high level of succinate and reduce acetate formation.....	17
2.7 Glucose and xylose metabolism pathway in <i>E. coli</i> KJ12201.....	19
2.8 Typical cell growth curve.....	20
2.9 The effect of residual growth-limiting substrate on specific growth rate.....	23
4.1 The cell concentration profiles of <i>E. coli</i> KJ12201 at different initial xylose concentrations.....	41
4.2 The cell concentration profiles of <i>E. coli</i> KJ12201 at different initial glucose concentrations.....	41
4.3 The xylose consumption profiles of <i>E. coli</i> KJ12201 at different initial xylose concentrations.....	43
4.4 The glucose consumption profiles of <i>E. coli</i> KJ12201 at different initial glucose concentrations.....	43

LIST OF FIGURES (Continued)

Figure	Page
4.5 The succinate production profiles of <i>E. coli</i> KJ12201 at different initial xylose concentrations.....	45
4.6 The acetate production profiles of <i>E. coli</i> KJ12201 at different initial xylose concentrations.....	45
4.7 The succinate production profiles of <i>E. coli</i> KJ12201 at different initial glucose concentrations.....	46
4.8 The acetate production profiles of <i>E. coli</i> KJ12201 at different initial glucose concentrations.....	46
4.9 The relative specific growth rate of <i>E. coli</i> KJ12201 at different initial succinate concentrations of xylose consumption.....	49
4.10 The relative specific growth rate of <i>E. coli</i> KJ12201 at different initial succinate concentrations of glucose consumption.....	49
4.11 The specific growth rate of <i>E. coli</i> KJ12201 at different initial xylose concentrations.....	51
4.12 The specific growth rate of <i>E. coli</i> KJ12201 at different initial glucose concentrations.....	51
4.13 The relationship between %change of function $f(pp)$ on (a) 5% increase and (b) decrease of each parameter value in model prediction of xylose.....	57
4.14 The relationship between %change of function $f(pp)$ on (a) 5% increase and (b) decrease of each parameter value in model prediction of glucose.....	58

LIST OF FIGURES (Continued)

Figure		Page
4.15	The experimental and model predicted profiles at initial substrate concentration of model calibration. Left and right panels for xylose and glucose, respectively.....	65
4.16	The experimental and model predicted profiles at initial substrate concentration of model validation. Left and right panels for xylose glucose, respectively.....	66



LIST OF ABBREVIATIONS

μ	=	Specific growth rate
μ_{\max}	=	Maximum specific growth rate
α_{acetate}	=	Growth associated term of acetate formation
$\alpha_{\text{succinate}}$	=	Growth associated term of succinate formation
β_{acetate}	=	Non-growth associated term of acetate formation
$\beta_{\text{succinate}}$	=	Non-growth associated term of succinate formation
C_{acetate}	=	Acetate concentration
C_{cell}	=	Cell concentration
C_{glucose}	=	Glucose concentration
$C_{\text{succinate}}$	=	Succinate concentration
$C^*_{\text{succinate}}$	=	Critical succinate concentration that completely inhibits cell growth
$C_{\text{substrate}}$	=	Substrate concentration
$C^*_{\text{substrate}}$	=	Critical substrate concentration that completely inhibits cell growth
C_{xylose}	=	Xylose concentration
C^*_{xylose}	=	Critical xylose concentration that completely inhibits cell growth
k_s	=	Monod constant or substrate saturation constant
$k_{i,s}$	=	Substrate inhibition constant
k_l	=	Cell lysis constant

LIST OF ABBREVIATIONS (Continued)

k_L	=	Cell lysis rate
$k_{l,max}$	=	Maximum rate of cell lysis
n	=	Power constant of substrate inhibition
m_e	=	Cell maintenance coefficient
OD_{550}	=	Optical density at 550 nm
q	=	Power constant of product inhibition
R^2	=	Coefficient of determination
t	=	Time
$Y_{cell/glucose}$	=	Production of cell to consumed glucose
$Y_{cell/xylose}$	=	Production of cell to consumed xylose
$Y_{succinate/glucose}$	=	Production of succinate to consumed glucose
$Y_{succinate/xylose}$	=	Production of succinate to consumed xylose
$Y_{acetate/glucose}$	=	Production of acetate to consumed glucose
$Y_{acetate/xylose}$	=	Production of acetate to consumed xylose
σ^2	=	Measurement of the spread between numbers in a data set, Variance

CHAPTER I

INTRODUCTION

1.1 Rationale of the Study

Succinate or succinic acid is one of the building-block chemicals that can be produced by both petrochemical and fermentative processes and is a widely versatile chemical for being reactive substrates as additives, pharmaceutical agents, surfactants, and intermediates (Cukalovic et al., 2008). The competition trend of succinate production between petrochemical process and bio-based fermentation is predictable regarding to its sustainability and productivity. However, the bio-based process is an accomplished competitor that can replace the petrochemical process. Furthermore, the bio-based succinate production can be improved to obtain high productivity with less production cost by optimizing the fermentative process (Pinazo et al., 2015).

The optimizations of succinate fermentation have been extensively developed in several strategies including genetic modification of microorganisms, improvements of fermentative process and equipment design as well as a suitable utilization of fermentative substrates. Normally, succinate can be produced under anaerobic conditions by various wild type microorganisms. Afterward, many relative succinate production genes have been studied to find the optimum route for producing high succinate in several microorganisms.

Genetic engineered microorganisms have been examined to investigate their ability of succinate production in many conditions. *Actinobacillus succinogenes* produced succinate from fruit and vegetable wastes(FVW) hydrolysate (Dessie et al., 2018) . *Basfia succiniciproducens* produced succinate from xylose- containing hydrolysates from corn stover (Salvachúa et al., 2016). Engineered yeast *Yarrowia lipolytica* produced succinic acid from glycerol (Li et al., 2017).

Owing to gene manipulation, clear genetic information, and high growth rate in minimal nutrient, *Escherichia coli* is an interesting selective microorganism that has been genetically modified for succinate production. Many reviews demonstrated the effectiveness of succinate related genes of *E. coli* (Zhu et al., 2017). *E. coli* KJ073 that had been genetically engineered from the parental strain *E. coli* C is considered as one of the promising succinate producers on glucose as a substrate (Jantama et al., 2008a). However, strain KJ073 produced succinate with many by-products including acetate, malate, and pyruvate. For further improvement, *E. coli* KJ073 had been metabolically evolved and further genetically modified to be *E. coli* KJ122 in order to produce higher succinate yield and concentration with less by-products (Jantama et al., 2008b). Lignocellulosic biomass is well known for a sustainable and renewable resource. A large amount of invaluable lignocellulosic biomass is discharged from the agricultural and industrial sectors. Nevertheless, lignocellulosic wastes contain xylose relative compounds including hemicelluloses. These can be converted to xylose as a monosaccharide which can be further used as a fermentative sugar substrate. For this reason, *E. coli* KJ122 was further engineered to improve the uptake rate and utilization of xylose by deleting *xylFGH* genes and was assigned to be *E. coli* KJ12201. The strain could produce higher succinate concentration and with a greater productivity from xylose than those of *E. coli* KJ122 (Khunnonkwao et al., 2018).

For determining the suitable conditions of succinate production by each succinate producer, collecting information concerning the growth rate, substrate consumption and product formation is necessary. This information is used to construct the mathematical models for estimating the succinate production on various conditions. Kinetic models of succinate production by *A. succinogenes* and *E. coli* were constructed based on glucose as a substrate in which succinate as a major product, and formate, acetate, lactate as by-products (Corona-González et al., 2008; Li et al., 2010). The model of succinate production was also constructed from glycerol utilization by *Actinobacillus succinogenes* (Vlysidis et al., 2011). Kinetic models of *Actinobacillus succinogenes* and *Basfia succiniciproducens* were formed on the xylose-based substrate corresponding to a spent sulphite liquor (Pateraki et al., 2016).

The ability of succinate production by *E. coli* KJ12201 could be considerably more challenging when lignocellulosic biomass is used as a substrate. Lignocellulosic biomass is readily available in Thailand. It is an agricultural waste that is usually abundant and is buried or burnt. However, it contains hemicellulose structure that can be converted into fermentable sugars for succinate production. Therefore, this study focused on evaluating succinate production from fermentable sugars (xylose and glucose) which are the main components in lignocellulosic biomass and constructing the kinetic model in fermentation process by *E. coli* KJ12201. The kinetic model was constructed to investigate effects of varying substrate and product concentrations on growth and product formation of *E. coli* KJ12201. The kinetic growth rate was based on Monod, Haldane-Andrews, Levenspiel, Aiba-Edward, and Teissier models. The developed model was then calibrated to obtain the kinetic parameters by MATLAB software to precisely apply for predicting fermentation performances.

1.2 Research objectives

Presently, the direction of sustainable industry and environmental-friendly process is considerable. Therefore, the strain that can consume xylose and glucose such as *E. coli* KJ12201 is an interesting alternative for the industrial succinate production. *E. coli* KJ12201 was kinetically evaluated under cultivating on various concentrations of individual xylose and glucose. The kinetic models were constructed based on xylose and glucose fermentation using MATLAB software.

The main of project objectives were

1. To evaluate effects of various initial xylose, glucose, and succinate concentrations on cell growth, substrate consumption, and succinate production by *E. coli* KJ12201 in batch fermentation under anaerobic conditions
2. To construct an unstructured mathematical kinetic model representing results on growth rate, substrates consumption, and product formation by estimating key kinetic parameters which rely on descriptions of substrate and product inhibition

1.3 Scope and limitations

The AM1 mineral salt, 1M Betaine-HCl, and 100 mM KHCO₃ were together used as a cultivation medium. The synthetic media containing glucose and xylose were separately applied for analyzing the influence of substrate concentrations. Additionally, the synthetic medium containing succinate at different concentrations were used in part of effects for product concentrations. To apply the model for predicting at various initial substrate concentration therefore yield of cell, succinate, and acetate that were proposed in model were assumed to be constant. The acetate inhibition was neglectable in this study due to its less amount produced by *E. coli* KJ12201.

CHAPTER II

REVIEW OF THE LITERATURE

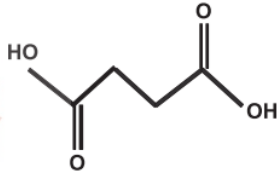
2.1 Succinate applications and its production

Succinate or succinic acid is a member of C₄-tricarboxylic acid family and is a conventional name of butanedioic acid with the chemical formula (CH₂)₂(CO₂H)₂. The physical and chemical properties of succinate are illustrated in **Table 2.1**. The succinate is a one of most promising fermentation products. It is an intermediate chemical of tricarboxylic acid (TCA) cycle in the cell. Traditionally, succinate is well-known as “amber acid” which was purified by using distillation processing to extract the amber into succinate and other chemical compounds (Saxena et al., 2017). Nowadays, succinate is commercially produced via petrochemical and fermentation processes. Its advantages have been found in various applications for producing many commercial products such as surfactants, food additives, chelators in the industries of pharmaceutical, agricultural, and food industries. It is also used as a starting chemical for polymerizing or transforming into commodity chemicals including 1,4 butanediol, adipic acid, 2-pyrrolidinone, and diethyl succinate. Moreover, the United States Department of Energy termed succinate as one of the promising 12 bio-based building blocks (**Figure 2.1**) (Werpy et al., 2004). These succinate-derived products are summarized as shown in **Figure 2.2**.

Building Blocks
1,4 succinic, fumaric and malic acids
2,5 furan dicarboxylic acid
3 hydroxy propionic acid
aspartic acid
glucaric acid
glutamic acid
itaconic acid
levulinic acid
3-hydroxybutyrolactone
glycerol
sorbitol
xylitol/arabinitol

Figure 2.1 The twelve sugar-based building blocks (Werpy et al., 2004).

Table 2.1 Physical and chemical properties of succinate (Saxena et al., 2017).

Succinic acid also know as	amber acid; butanedioic acid; dihydrofumaric acid; asuccin; bernsteinsäure; kyselina jantarova	 <p>Structural Formula of Succinic Acid</p>
IUPAC name	Butanedioic acid	
Molecular formula	$C_4H_6O_4(HOOCCH_2CH_2COOH)$	
Physical state	Colorless, odorless white crystals	
Melting point	185–187°C	
Boiling point	235°C	
Solubility in solvents	Slightly dissolved in ethanol, ether, acetone, and glycerin; not dissolved in benzene, carbon sulfide, carbon tetrachloride, and oil ether	
Solubility in water	Soluble	
Molar mass	118.09	
Specific gravity	1.552	
Flash point	206°C	
Density	1.56 g/cm ³	
Vapor density	3.04	
Acidity (pK _a)	pK _{a1} = 4.2 pK _{a2} = 5.6	
Stability	Stable under ordinary conditions	
Occurrence	Naturally occurs in plant and animal tissues	
Applications	Pharmaceuticals, agriculture, food products, and other industrial uses	

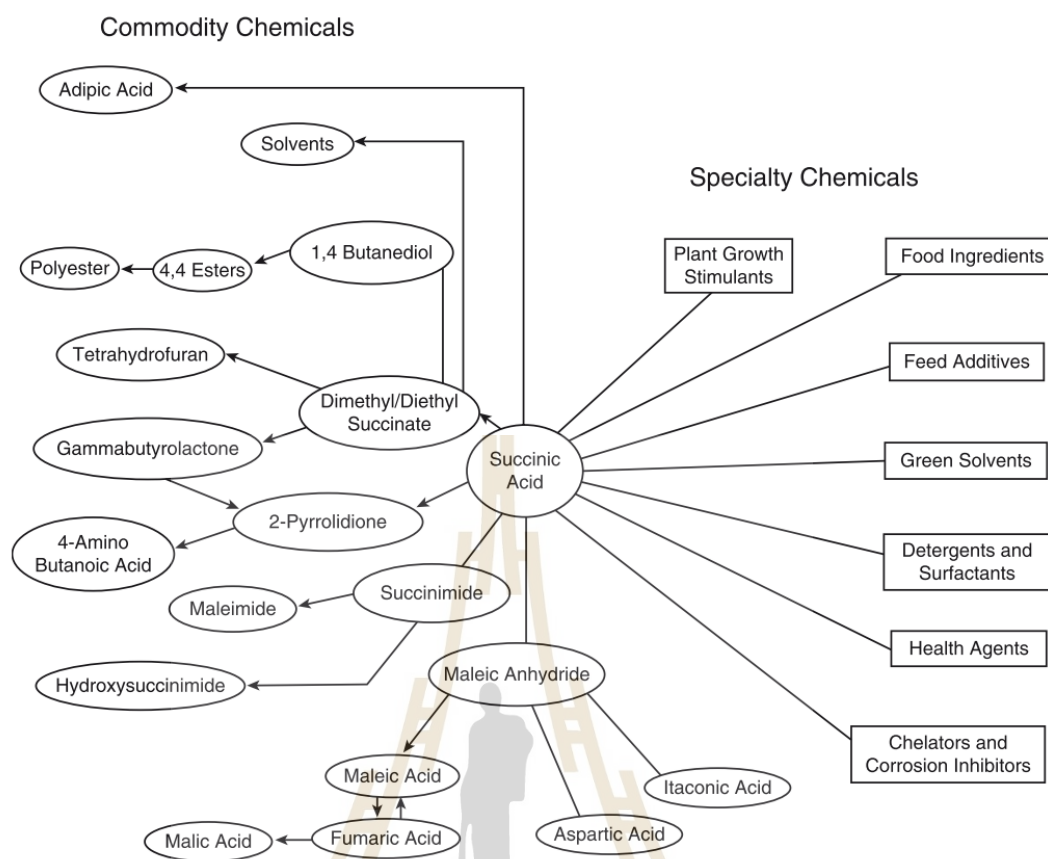


Figure 2.2 Chemicals and products derived from succinate (McKinlay et al., 2007).

The worldwide industrial production of succinate had significantly risen from 15,000 million tons in the year 1999, and up to 180,000 metric tons in year 2015 (**Figure 2.3**). The higher production of succinate is obtained from the fermentative process comparable to the petrochemical process. The comparative parameters as important factors for determining the suitable process for the succinate production were calculated including material and energy efficiencies, land usage, and total production cost. These four indicators demonstrate that bio-based process is an accomplished competitor that can replace the petrochemical process. Furthermore, the bio-based process can be improved to obtain high productivity and less production cost by optimizing the fermentative process (Pinazo et al., 2015).

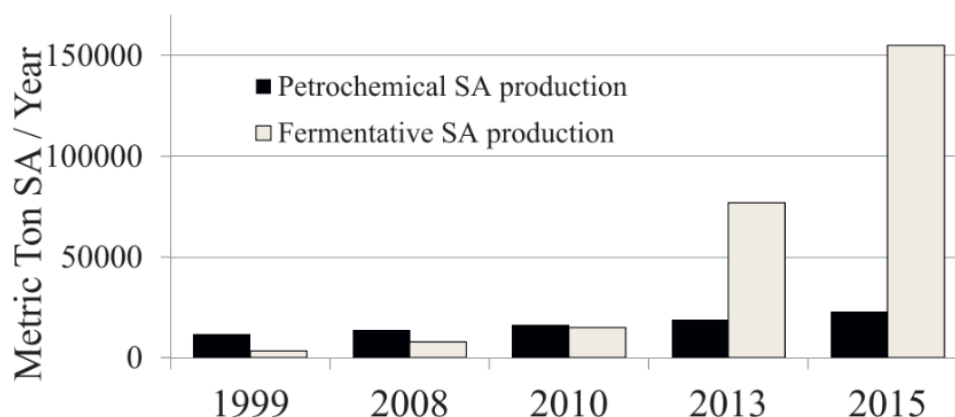


Figure 2.3 The increase of worldwide succinate production (Pinazo et al., 2015).

2.2 Succinate fermentation

The important factors for improving succinate fermentation are a kind of microbial fermentation, and sorts of sugar (Pinazo et al., 2015). Based on the theoretical chemical reaction, the maximum of succinate by converting of glucose into succinate in fermentative process *via* metabolic pathway in **Figure 2.4** can be expressed as



From the above equation, 1 mole of glucose is converted to 1.71 moles of succinate by reacting with 0.86 mole of bicarbonate, 1.74 moles of water and 2.58 moles of hydrogen ion are by-products from the reaction.

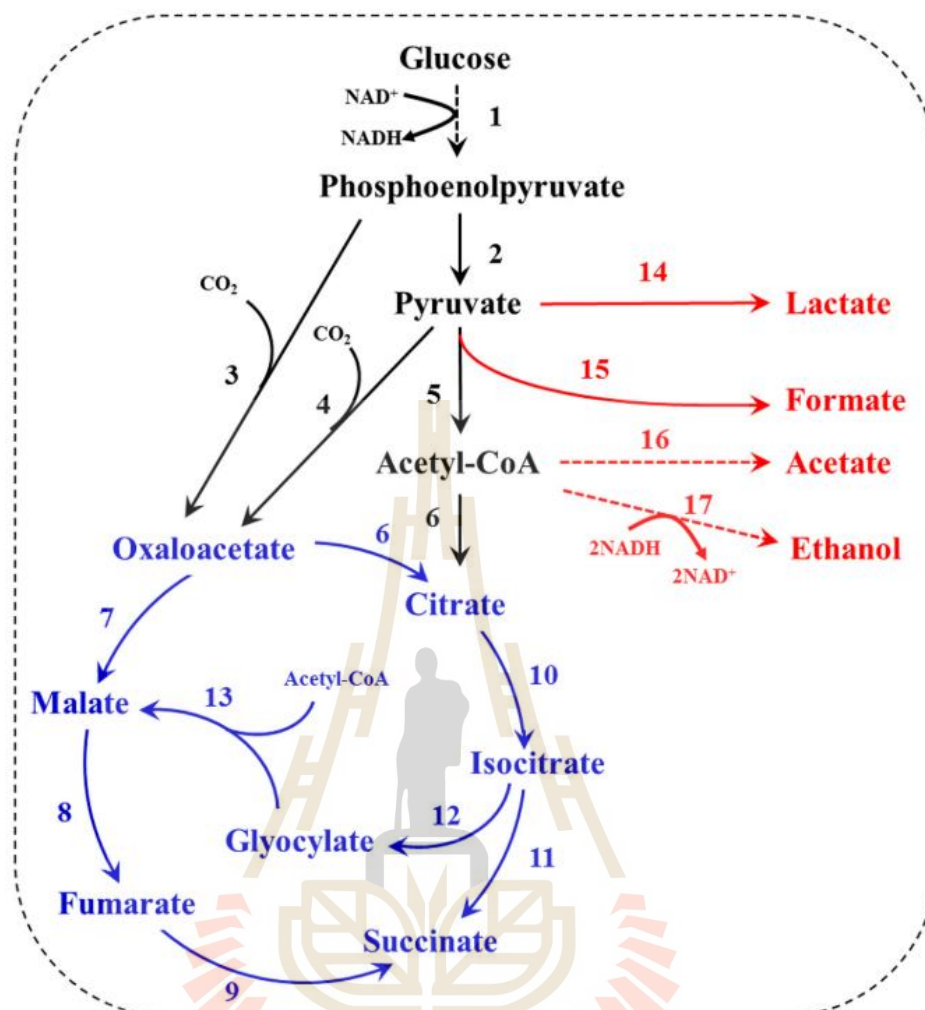


Figure 2.4 Succinic acid production pathways in microorganism (Jiang et al., 2017).

(1) Embden-Meyerhof pathway enzymes; (2) pyruvate kinase; (3) phosphoenolpyruvate carboxylase; (4) pyruvate carboxylase; (5) pyruvate dehydrogenase; (6) citrate synthase; (7) malate dehydrogenase; (8) fumarase; (9) fumarate reductase; (10) aconitase; (11) isocitrate lyase; (12) isocitrate lyase; (13) malate synthase; (14) lactate dehydrogenase; (15) pyruvate-formate lyase; (16) phosphor-transacetylase and acetate kinase; (17) acetaldehyde dehydrogenase and alcohol dehydrogenase.

The promising strains of microbial fermentation for being potential succinate producers are summarized separately as following; *A. succinogenes* (**Table 2.2**), *Corynebacterium glutamicum* (**Table 2.3**), *E. coli* (**Table 2.4**), *Mannheimia succiniciproducens* (**Table 2.5**), and *Saccharomyces cerevisiae* (**Table 2.6**).

The characteristics and living conditions of each microbial strain during succinate production in **Table 2.2** to **Table 2.6** were noticeably different. *A. succinogenes* synthesizes succinate as a natural primary product nevertheless this strain cannot tolerate high concentration of succinate and was not extensively metabolically engineered (Li et al., 2010). *M. succiniciproducens* produced succinate as a major product in facultative aerobic conditions but it is auxotrophic with amino acid and vitamin (Song et al., 2008). *C. glutamicum* can utilize a board spectrum of carbon source. However, *C. glutamicum* does not grow under anaerobic conditions. *S. cerevisiae* cannot normally produce succinate at high concentration thus it has to be developed via genetic engineering to enhance succinate production. For *E. coli*, it has been widely studied for producing succinate because of its high growth rate and clear genetic information, and it possesses simple techniques for gene manipulation and minimal nutrient requirement (Zhu et al., 2017).

Table 2.2 Succinate production by *A. succinogenes*.

Strain	Substrate	Conditions	Concentration (g/L)	Productivity (g/L/h)	Yield (g/g)	References
<i>A. succinogenes</i>						
130Z	Deacetylated DAP hydrolysate	Anaerobic, batch	42.80	1.27	0.74	(Salvachua et al., 2016)
130Z	Corn stover hydrolysate stream	Anaerobic, continuous fermentation	39.60	1.77	0.78	(Bradfield et al., 2015)
130Z-pMDH	Glucose and xylose	Anaerobic, batch	34.20	0.58	0.36	(Guarnieri et al., 2017)
CGMCC 1716	Corn fiber hydrolyzate	Anaerobic, batch	35.40	0.98	0.73	(Chen et al., 2010)
CIP 106512	Sugarcane bagasse hemicellulose hydrolysate	Anaerobic, batch	22.50	1.01	0.43	(Borges et al., 2011)

Table 2.3 Succinate production by *C. glutamicum*.

Strain	Substrate	Conditions	Concentration (g/L)	Productivity (g/L/h)	Yield (g/g)	References
<i>C. glutamicum</i>						
BOL-3/pAN6-gap	Glucose	Dual phase, fed batch	133.8	2.48	1.09	(Litsanov et al., 2012)
Δ ldhA-pCRA717	Glucose	Microaerobic, fed batch	146	3.17	0.92	(Okino et al., 2008)
R(DldhApCRA717)	Glucose	Micro-aerobic, fed batch with membrane for cell recycling	146	3.17	0.92	(Okino et al., 2008)
ZX1 (pEacsAgltA)	Glucose	Aerobic, bed-batch	28.5	0.39	0.41	(Zhu et al., 2013)

Table 2.4 Succinate production by *E. coli*.

Strain	Substrate	Conditions	Concentration (g/L)	Productivity (g/L/h)	Yield (g/g)	References
<i>E. coli</i>						
AFP111	Glucose	Dual phase, fed batch	101.2	1.89	1.07	(Jiang et al., 2010)
AS1600a	Mixture of xylose and glucose	Anaerobic, batch	84.26	0.96	0.88	(Sawisit et al., 2015)
HX024	Glucose	Anaerobic, batch	95.9	0.89	-	(Zhu et al., 2014)
KJ060	Glucose	Anaerobic, batch	86.5	0.9	0.93	(Jantama et al., 2008a)
KJ122	Glucose	Anaerobic, batch	83.00	0.88	0.90	(Jantama et al., 2008b)
KJ12201	Mixture of xylose and glucose	Anaerobic, batch	70.80	0.58	0.87	(Khunnonkwao et al., 2018)
SD121	Glucose	Dual phase, fed batch	116.2	1.55	1.13	(Wang et al., 2011)
Tang1527	Glucose	Dual phase, batch	89.4	1.24	1.27	(Yu et al., 2016)
YL106/pSCsfca	Glucose	Aerobic-microaerobic anaerobic phase, fed batch	85.3	2.13	0.65	(Li et al., 2013)

Table 2.5 Succinate production by *M. succiniciproducens*.

Strain	Substrate	Conditions	Concentration (g/L)	Productivity (g/L/h)	Yield (g/g)	References
<i>M. succiniciproducens</i>						
MBEL55E	Glucose	Anaerobic, batch	10.50	1.75	0.59	(Song et al., 2007)
LPK7	Glucose	Anaerobic, fed batch	52.40	1.75	0.76	(Lee et al., 2006)

Table 2.6 Succinate production by *S. cerevisiae*.

Strain	Substrate	Conditions	Concentration (g/L)	Productivity (g/L/h)	Yield (g/g)	References
<i>S. cerevisiae</i>						
AH22ura3	Glucose	Aerobic, batch	3.62	0.022	0.072	(Raab et al., 2010)
PMCFfg	Glucose	Aerobic, batch	12.97	0.11	0.13	(Yan et al., 2014)

E. coli KJ12201 was modified from strain KJ122 that was successively developed from the parental *E. coli* C (**Figure 2.5**). At the beginning, *E. coli* KJ073 was developed from *E. coli* C by deleting genes related to the central anaerobic fermentation (*ldhA*, *adhE*, *ackA*, *focA-pflB*, *mgsA*, *poxB*). After that, it was metabolically evolved for selecting the mutant cell that could produce higher succinate. Succinate production by that mutant cell was around 1.2 moles of succinate per mole of consumed glucose and then, the mutant cell was nominated as *E. coli* KJ073 (Jantama et al., 2008a). However, *E. coli* KJ073 was remained residual recombinase sites (FRT sites) on its genome. Subsequently, all FRT sites on the strain were substituted by native DNA containing the designed deletion, and the final strain was designed as *E. coli* KJ091 (Jantama et al., 2008b).

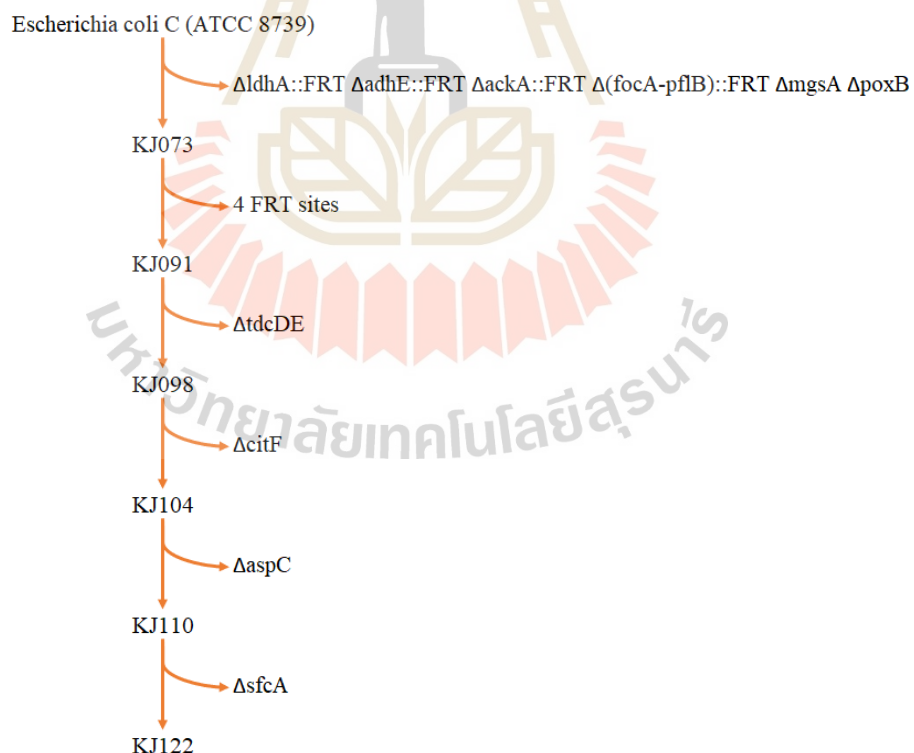


Figure 2.5 Construction steps of strain KJ122 from the parental *E. coli* C (Jantama et al., 2008b).

The acetate production was proved in strain KJ091 that it suppressed the succinate yields under anaerobic fermentation of glucose via a conversion pathway of acetyl CoA to acetate. The alteration level of acetyl-CoA represents the changing of succinate yield. Therefore, the formation pathway of acetyl-CoA from pyruvate by using pyruvate formate-lyase (*pflB*) and acetate from acetyl-P by using acetate kinase (*ackA*) were originally eliminated in the strain. In addition, *tdcD* gene that is an alternative gene encoding acetate kinase activity under anaerobic conditions and *tdcE* gene encoding pyruvate formate-lyase activity were deleted from *E. coli* KJ091 to design *E. coli* KJ098. For *E. coli* KJ098, the succinate yield increased about 10%, acetate production reduced about 42% as well as the level of pyruvate also reduced about 40% compared with those of *E. coli* KJ091 (Jantama et al., 2008b).

citF was further deleted from strain KJ098 to design KJ104, and *aspC* was deleted from strain KJ104 to design KJ110, both *citF* and *aspC* have no effect on succinate yield. On the other hand, the deletion of combined *aspC* and *sfcA* genes had an effect on an increase in succinate yield, succinate titer, and succinate productivity of 8%, 13%, and 14%, respectively in strain KJ122 compared to those of the parental strain KJ104. The final strain KJ122 produced succinate at 85% of maximum theoretical yield (1.71 mol per mol glucose) that was 1.4 - 1.5 mol succinate per mol glucose or 0.984 gram-succinate per gram-glucose, titer (700 mM), and average productivity (0.9 g/L/h) from 10%(w/v) glucose (Jantama et al., 2008b). The overall improvements of strain KJ073 to KJ122 by genes deletion are illustrated as in **Figure 2.6**.

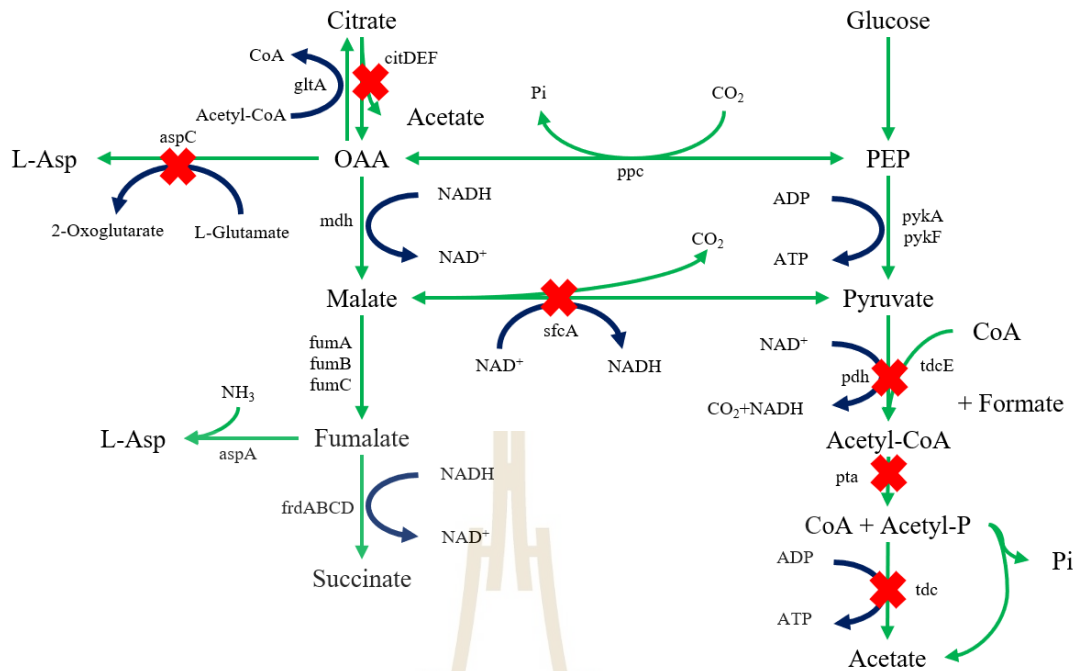


Figure 2.6 Genes deletion of *E. coli* strain KJ073 to design KJ122 for producing high level of succinate and reduce acetate formation. Relevant genes and enzymes are abbreviated as following: *citDEF*, citrate lyase; *gltA*, citrate synthase; *aspC*, aspartate aminotransferase; *aspA*, aspartate ammonia lyase (malate); *ppc*, phosphoenolpyruvate carboxylase; *sfcA*, NAD⁺-linked malic enzyme; *fumA* & *fumB*, fumarase; *frdABCD*, fumarate reductase; *pykA* & *pykF*, pyruvate kinase; *tdcE*, pyruvate formate-lyase (homologue of *pflB*); *pta*, phosphoacetyltransferase; *tdcD*, propionate kinase (analogous function to *ackA*); *pflB*, pyruvate formate-lyase; and *ackA*, acetate kinase. Crossed signs represent deletion of genes in *E. coli* KJ122 strain (Jantama et al., 2008b).

E. coli KJ122 successfully achieves succinate production on glucose as a substrate; nevertheless, on sole xylose, the strain KJ122 existed long lag phase (around 48 hours) and xylose was slowly consumed. Succinate yield and productivity of 0.67 ± 0.02 g/g and 0.26 ± 0.01 g/L/h, respectively, at 10% (w/v) xylose were less than those of at 10% (w/v) glucose. Since catabolic pathway of xylose produces only 0.67 ATP *via* pentose phosphate pathway in *E. coli* (Hasona et al., 2004), the xylose transportation *via* ABC transporter and xylose phosphorylation generally required 2 ATP thus resulting in an insufficient ATP production in *E. coli* KJ122 (Khunnonkwao et al., 2018) during succinate production. The *xylFGH*, ATP- dependent xylose transporter genes were deleted from the strain KJ122 to design the strain KJ12201 (**Figure 2.7**). It evidently indicated that more xylose was efficiently consumed. Strain KJ12201 produced succinate concentration (70.8 ± 3.4 g/L) and succinate productivity (0.58 ± 0.02 g/L/h) higher than those of strain KJ122 at the end of fermentation in the medium containing 10% (w/v) xylose (Khunnonkwao et al., 2018).

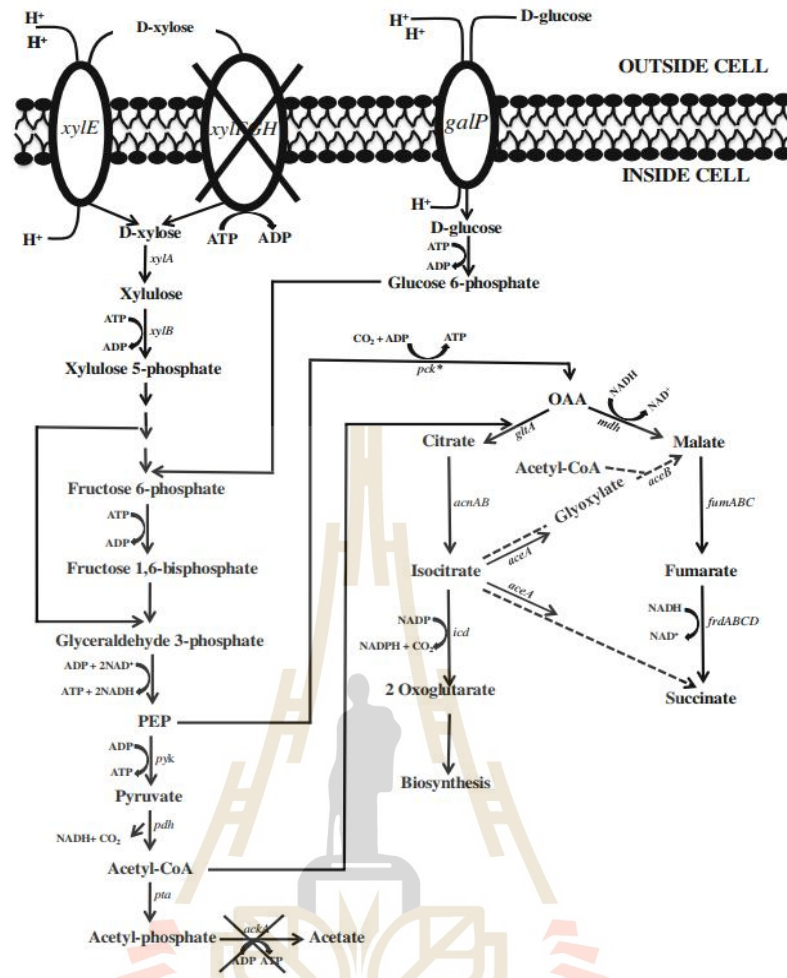


Figure 2.7 Glucose and xylose metabolism pathway in *E. coli* KJ12201.

Nomenclatures for genes and enzymes: *galP*, galactose permease; *xylE*, D-xylose::H⁺ transporter; *xylFGH*, ATP-dependent xylose transporter; *xylA*, xylose isomerase; *xylB*, xylulokinase; *pyk*, pyruvate kinase; *pta*, phosphate acetyltransferase; *ackA*, acetate kinase; *gltA*, citrate synthase; *mdh*, malate dehydrogenase; *fumABC*, fumarase; *frdABCD*, fumarate reductase; *aceA*, isocitrate lyase; *aceB*, malate synthase A; *acnAB*, aconitase; and *icd*, isocitrate dehydrogenase; *pck**, a spontaneous mutation in *pck* gene hence approving the enzyme to serve as the primary route for oxaloacetate production; *pdh*, pyruvate dehydrogenase. Crossed signs represent deletion of genes in *E. coli* KJ12201 strain (Khunnonkwao et al., 2018)

2.3 Batch fermentation kinetics

The fermentation operations are usually applied in various kind of products. The common type of the closed fermentation system is batch operation. The cell inoculum will pass through a number of phases (Natarajan, 2018) as shown in **Figure 2.8**. A few cell growth phases under typical batch operation generally are 1) lag phase, 2) logarithm or exponential phase, 3) deceleration phase, 4) stationary phase, and 5) death phase. Microbial cell growth is a consequence of cell activities such as cell replication, cell's size changing as well as the substrate utilization under various cultivated parameters of physical, chemical, and nutritional conditions. The microbial cell uptakes nutritional substrates and converts these substrates to produce energy or to use for biosynthesis for product formation.

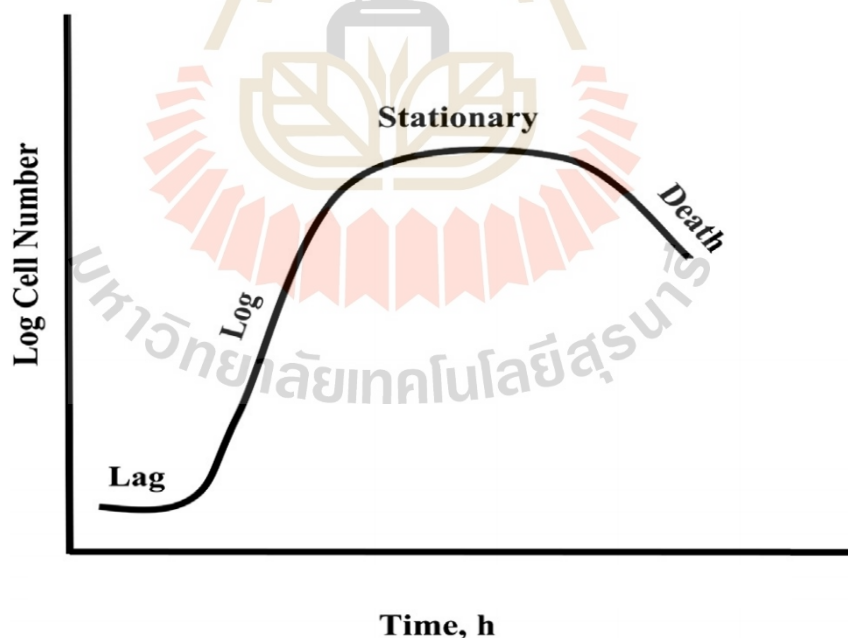


Figure 2.8 Typical cell growth curve (Natarajan, 2018).

Phase kinetics of cell growth curve as presented in **Figure 2.8** can be described as following.

- Lag phase is the first period of microbial cell growth. At the beginning, the microbial cell adapts itself after transferring into the new medium. This phase has no cell growth therefore the cell concentration is usually constant. A decrease in the lag phase is important to reduce the fermentation time.
- Exponential phase or log phase exhibits in growth curve after the microbial cell is adapted. This phase indicates the cell growth rate of organism. An increase in the cell concentration relies on the initial cell concentration and can be described as

$$\frac{dC_{\text{cell}}}{dt} \propto C_{\text{cell}} \quad \text{Eq. (2.2)}$$

Where C_{cell} is cell concentration (g-cell/L)

t is fermentation time (h)

The account of cell concentration in exponential phase is added the specific growth rate (μ) and changes into the new equation form as

$$\frac{dC_{\text{cell}}}{dt} = \mu C_{\text{cell}} \quad \text{Eq. (2.3)}$$

Where μ is the specific growth rate that is the produced cell concentration per cell concentration and fermentation time (g- cell /(g-cell-h)).

The cell growth rate gradually increases until the maximum cell growth rate is reached. At maximum cell growth rate (μ_{max}), biomass concentration increases rapidly due to the excess substrate concentration under that of fermentation condition. Therefore, the maximum cell growth rate relies on many factors such as the sort of

substrate, substrate and medium composition, pH, and temperature (Stanbury et al., 2017).

- Deceleration and stationary phases are illustrated after the exponential phase. At the end of exponential phase, the specific cell growth rate decreases due to the influence of the residual amount of some essential substrates, the accumulation of toxic products or combination of both (Stanbury et al., 2017).
- Death phases exhibited after the stationary phases. The cell lysis occurs due to the stress (Rigaki et al., 2020) and the accumulation of toxic. The expression of death phase can be described by term of cell lysis rate (Rigaki et al., 2020).

$$k_L = k_{L,\max} \left(\frac{k_1}{C_{\text{substrate}} + k_1} \right) \quad \text{Eq. (2.4)}$$

Where k_L is cell lysis rate (1/h)

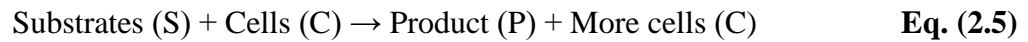
$k_{L,\max}$ is maximum rate of cell lysis (1/h)

k_1 is lysis constant (g/L)

$C_{\text{substrate}}$ is substrate concentration (g-substrate/L)

2.4 Fundamental unstructured growth kinetic model

The overall growth phenomenon can be considered as a basic reaction with a simple rate expression even though the growth of microbial cell is a complicated phenomenon (Han et al., 1988). Monod equation is a traditional growth kinetic model that describes the relationship between specific growth rate (μ) and the residual growth-limiting substrate (s) as illustrated in **Figure 2.9**. This equation is usually applied to the decrease and cessation of cell growth due to the depletion of substrate (Stanbury et al., 2017).



$$\frac{r_{\text{cell}}}{C_{\text{cell}}} = \mu = \mu_{\text{max}} \left[\frac{C_{\text{substrate}}}{C_{\text{substrate}} + k_s} \right] \quad \text{Eq. (2.6)}$$

Where r_{cell} is growth rate of cells (g-cell/L/h)

μ_{max} is maximum specific growth rate (1/h)

μ is specific growth rate (1/h)

$C_{\text{substrate}}$ is substrate concentration (g-substrate/L)

k_s is Monod constant (g-substrate/L)

C_{cell} is cell concentration (g-cell/L)

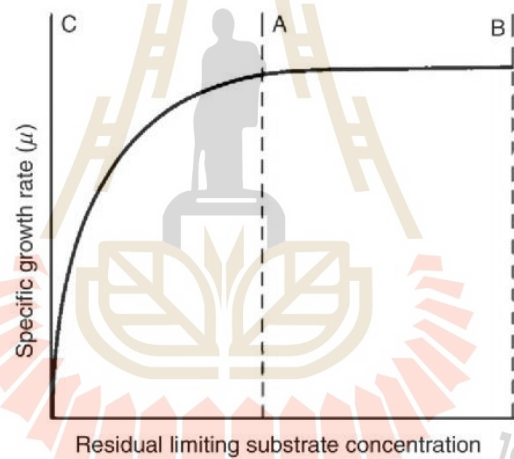


Figure 2.9 The effect of residual growth-limiting substrate on specific growth rate (Stanbury et al., 2017).

The relationship between residual growth-limiting substrate and specific growth rate indicates the two zones of phenomenon (Stanbury et al., 2017).

Zone A to B shows an exponential phase of microbial growth. This zone exhibits the maximum specific cell growth rate.

Zone C to A shows a deceleration phase. The cell growth rate is affected by a decrease in substrate to growth-limiting substrate concentration that is not support μ_{max} .

- For high affinity with limiting substrates (Low k_s value). The vary low substrate concentration affects cell growth rate so the deceleration phase is a short period.
- For low affinity with limiting substrates (High k_s value). The cell growth rate is influenced at high level of substrate concentration. This scenario exhibits the long period of the deceleration phase.

Generally, the proportional concentration of cell to substrate concentration can be described as

$$\frac{dC_{\text{cell}}}{dt} = \mu C_{\text{cell}} = \mu_{\text{max}} \left[\frac{C_{\text{substrate}}}{C_{\text{substrate}} + k_s} \right] C_{\text{cell}} \quad \text{Eq. (2.7)}$$

Where C_{cell} is cell concentration (g-cell/L)

μ is specific growth rate (1/h)

t is time (h)

The Monod equation is appropriate when the cell is cultivated on single substrate. Considering the two of different substrates, if those are required substrates for cell growth, the relationship between cell growth rate and co-substrate concentration can be explored as (Tampion, 1989)

$$\mu = \mu_{\text{max}} \left[\frac{C_1}{C_1 + k_{s,1}} \right] \left[\frac{C_2}{C_2 + k_{s,2}} \right] \quad \text{Eq. (2.8)}$$

Where subscript 1 and 2 represents the number of substrates

On the other hand, the independent substrate utilization can be described in different model because the cell can grow under the situation that lacks either one of the substrates. The general model for independent substrate utilization can be described as follow (Lee et al., 1995).

$$\mu = \mu_{\max,1} \left[\frac{C_1}{C_1 + k_{s,1}} \right] + \mu_{\max,2} \left[\frac{C_2}{C_2 + k_{s,2}} \right] \quad \text{Eq. (2.9)}$$

Where subscript 1 and 2 represents the number of substrates.

2.5 Kinetics for substrate and product inhibition

To determine the performance of the fermentation process, various key factors are the essential part. Those are not only process conditions but also the inhibition of substrate and product concentrations. The inhibition of bacterial growth by substrates or products can be usually explored at the extreme concentration. Additionally, when the excess of substrate is available, the inhibition can be exhibited under natural condition (Van Den Heuvel et al., 1988). Moreover, the presumable mechanisms of inhibition effect can be 1) an excess substrate by osmotic dehydration of the cell 2) organic acids by disrupting the intercellular pH (Edwards, 1970). The substrate is the essential factor for cell growth or other metabolic activities. At the extremely high concentration of substrate, it causes the defective physiological factors including the progressive loss in cell viability and cellular functions (Edwards, 1970). The kinetics of substrate inhibition can be widely described by various mathematical models. Kinetic models express the inhibitory effect of substrate on cell growth rate. The objective of each kinetic model has significantly developed for several presumptions. The general model of substrate inhibition on growth kinetics is concluded as following.

The Monod model had been proposed for the influence of a substrate inhibition by adding term of an inhibitory effect of substrate. The term of an inhibitory effect of substrate was presumably corresponded to the inhibition mechanism of products of the Levenspiel model (Levenspiel, 1980; Luong, 1987). Maximum substrate concentration, $C_{\text{substrate}}^*$, which cell is completely inhibited has been accounted.

$$\text{The Monod model : } \mu = \mu_{\max} \left[\frac{C_{\text{substrate}}}{k_s + C_{\text{substrate}}} \right] \left(1 - \frac{C_{\text{substrate}}}{C_{\text{substrate}}^*} \right)^n \quad \text{Eq. (2.10)}$$

The Haldane- Andrews model is usually used for describing the substrate inhibition at the high concentration (Andrews, 1968).

$$\text{The Haldane-Andrews model: } \mu = \mu_{\max} \left[\frac{C_{\text{substrate}}}{k_s + C_{\text{substrate}} + \frac{C_{\text{substrate}}^2}{k_{i,s}}} \right] \quad \text{Eq. (2.11)}$$

This model was developed based on describing the formation of an inactive enzyme-substrate complex with two substrate molecules. The model introduces a substrate inhibition parameter, $k_{i,s}$. Due to its simplicity and small number of parameters to be estimated, the Haldane-Andrews model is the most popular equation for substrate inhibition kinetics (Sadhukhan et al., 2016).

The kinetic model for correlating product inhibition of alcoholic fermentation was developed (Aiba et al., 1968). Then, the mechanism of product inhibition from Aiba model was proposed to correlate the substrate inhibition as following (Edwards, 1970). However, the Aiba-Edward model cannot predict the maximum substrate concentration.

$$\text{The Aiba-Edward model: } \mu = \mu_{\max} \left[\frac{C_{\text{substrate}}}{k_s + C_{\text{substrate}}} \right] e^{-\frac{C_{\text{substrate}}}{k_{i,s}}} \quad \text{Eq. (2.12)}$$

The cell growth is inhibited not only at the high substrate concentration, but also the other mechanisms. The kinetic model of diffusion-controlled substrate was firstly initiated by Teissier. The Teissier model was additionally developed by combining this mechanism with a protective diffusional limitation of high and inhibitory substrate concentrations (Edwards, 1970). The developed model of Teissier is expressed as following.

$$\text{The Teissier model: } \mu = \mu_{\max} \left(e^{-\frac{C_{\text{substrate}}}{k_{i,s}}} - e^{-\frac{C_{\text{substrate}}}{k_s}} \right) \quad \text{Eq. (2.13)}$$

Where μ is specific growth rate (1/h)

μ_{\max} is maximum specific growth rate (1/h)

$C_{\text{substrate}}$ is substrate concentration (g-substrate/L)

$C_{\text{substrate}}^*$ is critical substrate concentration (g-substrate /L)

C_{cell} is cell concentration (g-cell/L)

k_s is substrate saturation constant (g-substrate/L)

$k_{i,s}$ is substrate inhibition constant (g-substrate/L)

n is a constant

Considering the product formation, the accumulation of products during the fermentation usually can act as inhibition factors and decrease the cell growth rate (Vlysidis et al., 2011). Therefore, expression of specific cell growth rate with product inhibition can be described as a following equation (Levenspiel, 1980).

$$\mu_{\text{product}} = \mu_{\max} \left(1 - \frac{C_{\text{product}}}{C_{\text{product}}^*} \right)^p \quad \text{Eq. (2.14)}$$

Where μ_{product} is the specific growth rate (1/h)

μ_{\max} is the maximum specific growth rate (1/h)

C_{product} is the product concentration (g-product /L)

C_{product}^* is the critical product concentration (g-product /L)

p is a constant

Other equations of inhibition modelling also have been proposed in account of inhibition in which they are modified models derived from Monod equation to fit on various characteristics of specific growth rate. Consequently, the selection of growth

kinetic modelling depends on characteristics of relationship of specific growth rate to initial inhibitor concentrations (Han et al., 1988).

The kinetic models of succinate fermentation have been available on different microorganism with various sugar sources. The substrate and product inhibitions for succinate fermentation under glucose as major substrate by *A. succinogenes* were described by an extended Monod model. The results showed that critical concentrations of acetate, ethanol, formate, pyruvate and succinate were 46, 42, 16, 74, and 104 g/L, respectively (Lin et al., 2008). To evaluate inhibitory effects of fermentation products on the growth of *A. succinogenes* 130ZT, *E. coli* NZN111, AFP111 and BL21 strains, the continuous logistic equation which was originally modified from Monod equation was also applied. The equation could predict that these strains of *E. coli* produced the succinate more effectively than *A. succinogenes* at high concentrations of the initial succinate concentration (Li et al., 2010). For glycerol as substrate by *A. succinogenes*, the modified Monod equation was substituted by the Haldane equation for explaining cell behavior under growth inhibition by increasing glycerol concentration (Vlysidis et al., 2011). The construction of kinetic models for predicting substrate and product inhibitions of both *A. succinogenes* and *B. succiniciproducens* on mixed substrates of C5 and C6 sugars corresponding to spent sulphite liquor indicated the highest succinate yield, final concentration, and productivity of 0.76 g/g, 26.0 g/L and 0.66 g/L/h for *B. succiniciproducens* and 0.69 g/g, 27.4 g/L and 0.60 g/L/h for *A. succinogenes*. From above published kinetic models, they illustrated advantages of the developed mathematic models that can be used for optimizing the absolute amount of substrate feedstock, predicting the output of interesting product as well as evaluating of production cost.

2.6 Rates of substrate consumption and product formation

Cell growth pattern had been obviously shown in two kinetic states as exponential state and stationary state. Most of bacterial cells grow and cell density increase rapidly at the exponential phase due to high uptake rate of substrates and bioconversion of substrates is elevated to synthesize the product by the metabolic pathway. On the other hands, changing viability of bacterial cells is quite constant in exponential state which affects the rate of substrate uptake and product synthesis. Consequently, rates of substrate consumption and product formation are associated on cell growth.

The utilization of each substrate and the formation of product in fermentation process are separately calculated under the two phase of cell growth. In the period of exponential phase, the cell concentration increasingly changes with fermentation time. The nomination of the growth-associated parameter in substrate utilization and product formation is essential. Concerning a stationary phase, the cell concentration is admissibly constant. So, the key parameter of this phase is non-growth associated parameter.

The product formation was described by Luedking–Piret model where α_{product} is the growth associated parameters of product (g- product /g-cell) and β_{product} is the non-growth associated parameters of product (Luedeking et al., 1959) as following.

$$\frac{dC_{\text{product}}}{dt} = \alpha_{\text{product}} \frac{dC_{\text{cell}}}{dt} + \beta_{\text{product}} C_{\text{cell}} \quad \text{Eq. (2.15)}$$

Regrading substrate consumption, substrate in batch fermentation is usually utilized for growing of cell mass, producing product, as well as supporting cell maintenance. A substrate balance for the polysaccharides fermentation may be written (Mulchandani et al., 1988) as;

$$-\frac{dC_{\text{substrate}}}{dt} = \left(\frac{1}{Y_{\text{cell/substrate}}}\right)\left(\frac{dC_{\text{cell}}}{dt}\right) + \left(\frac{1}{Y_{\text{product/substrate}}}\right)\frac{dC_{\text{product}}}{dt} + m_e C_{\text{cell}} \quad \text{Eq. (2.16)}$$

$$-\frac{dC_{\text{substrate}}}{dt} = \left(\frac{1}{Y_{\text{cell/substrate}}} + \frac{\alpha}{Y_{\text{product/substrate}}}\right)\left(\frac{dC_{\text{cell}}}{dt}\right) + \left(\frac{\beta}{Y_{\text{product/substrate}}} + m_e\right)C_{\text{cell}} \quad \text{Eq. (2.17)}$$

Where m_e is maintenance coefficient (g-substrate/g-cell/h)

$C_{\text{substrate}}$ is substrate concentration (g-substrate/L)

C_{product} is product concentration (g-product/L)

C_{cell} is cell concentration (g-cell/L)

$Y_{\text{cell/substrate}}$ is biomass yield based on substrate (g-cell/g-consumed substrate)

$Y_{\text{product/substrate}}$ is product yield based on substrate (g-cell/g-consumed substrate)

α is growth associated product formation (g-product/g-cell)

β is non-growth associated product formation (g-product/g-cell/h)

CHAPTER III

MATERIALS AND METHODS

3.1 Microbial strains and inoculum preparation

E. coli KJ12201 was obtained from Metabolic Engineering Research Unit, School of Biotechnology, Institute of Agricultural Technology, Suranaree University of Technology, Nakhon Ratchasima, Thailand. The microorganism was appropriately preserved in cryopreservation vials at -80°C containing mixture of 50% (v/v) glycerol solution, and 50% (v/v) Luria Bertani (LB) broth which is comprised of 1% w/v peptone, 0.5% (w/v) yeast extract, and 0.5% (w/v) sodium chloride. The microbial stock was gradually defrosted and then streaked on petri dish containing LB agar. The bacterial colony on petri dish was incubated in conical flask containing 100 mL LB broth which was covered with silicone sponge closure for aerobic operating at 37°C in an orbital shaker at 200 rpm for approximately 12-16 hours.

Subsequently, the microbial inoculum in LB broth was separately transferred into two vessels that were contained different substrates. One substrate was glucose and the other was xylose. Each vessel was composed of similar nitrogenous based medium containing AM1 mineral salt medium containing 100 mM KHCO₃, and 1 M Betaine-HCl. The inoculum size and fermentation conditions were controlled at an initial OD₅₅₀ of 0.1 with a working volume of 350 mL at 37°C, pH 7.0, agitation at 200 rpm.

3.2 Fermentation process and conditions

The triplicate fermentation experiments were used to examine the inhibitory effect on the cell growth of *E. coli* KJ12201 and succinate production based on varying concentrations of xylose, glucose, and succinate. The vessel contained AM1 mineral salt medium supplementing with 100 mM KHCO_3 , and 1 M Betaine-HCl was prepared. The inoculum size was controlled at an initial OD_{550} of 0.1 with a working volume of 350 ml.

3.2.1 Effect of substrate concentration

For analyzing the inhibitory effect of substrate, different initial substrate concentrations were added into vessels. The range of xylose and glucose concentrations was 20-80 g/L. Subsequently, *E. coli* KJ12201 inoculum was cultivated into each vessel that contained the corresponded substrate.

3.2.2 Effect of product concentration

Besides the substrate inhibition, the product inhibition also was evaluated at the low substrate concentration for avoiding the side effects from the substrate inhibition. Therefore, the initial substrate concentration of individual sugar was fixed at 20 g/L. The succinate that is a major fermentation product by *E. coli* KJ12201 was separately analyzed for its inhibition during xylose and glucose fermentation. The various initial concentration of succinate was separately added into the vessel in ranges of 8-40 g/L and 12-60 g/L for xylose and glucose fermentation, respectively.

Anaerobic fermentations were appropriately conducted under three steady conditions as following (i) a water bath was controlled at the fermentation temperature of 37°C, (ii) a mixture of a basic solution containing 3 M K_2CO_3 and 6 M KOH was used as a pH regulator at 7.0 (Jantama et al., 2008b), and (iii) an agitation was

constantly regulated a rotational speed at 200 rpm. All solutions were prepared separately for sterilization by autoclave at 121°C for 20 min. The fermentation in each experiment was conducted in triplicate and the frequency of removing sample was based on initial substrate concentrations to obtain elaborated and comprehensive fermentation data.

3.3 Biomass and metabolites analysis

The growth of *E. coli* KJ12201 was estimated by using spectrophotometer to measure OD₅₅₀ and it was converted to dry cell weight (DWC) by using the conversion factor for *E. coli*; 1.0 OD₅₅₀ = 333 mg of dry cell weight per liter (Khunnonkwao et al., 2018). Concentrations of xylose, glucose, succinate, and acetate were analyzed by using high performance liquid chromatography (HPLC) installed with refractive index detectors with a Bio-Rad Aminex HPX-87H ion exclusion column. The temperature of column and detector was constantly kept at 45°C and the mobile phase which is 4 mM sulfuric acid was controlled at the constant flow rate of 0.4 mL/min.

3.4 Fermentation parameter calculation

The fermentation related parameters are the succinate yield, the specific growth rate, the substrate consumption rate, and the metabolite production rate. The yield of cell mass ($Y_{\text{cell/substrate}}$), succinate ($Y_{\text{succinate/substrate}}$), and acetate ($Y_{\text{acetate/substrate}}$) were assumed to be constant. The yield was calculated by the maximum concentration of either cell mass, succinate, or acetate divided by the consumed concentration of corresponding substrate. The specific growth rate (μ) was calculated by dividing $\Delta \ln$ (cell concentration) to Δtime within the period of exponential growth phase.

3.5 Kinetic model development

During the fermentation, the microbial cell was changing throughout the process. The rate of cell concentration was generally described by the specific growth rate and cell concentration. The specific growth rate correlates to the substrate concentration. Generally, the relationship between the specific growth rate on initial concentration of substrate was expressed by Monod equation.

$$\text{Rate of cell growth: } \frac{dC_{\text{Cell}}}{dt} = \mu C_{\text{cell}} \quad \text{Eq. (3.1)}$$

$$\text{Monod model: } \mu = \mu_{\text{max}} \left[\frac{C_{\text{Substrate}}}{C_{\text{Substrate}} + k_s} \right] \quad \text{Eq. (3.2)}$$

Additionally, the other notable models (Haldane-Andrews, Monod, Aiba-Edward, and Teissier model) were proposed in this study for describing the inhibitory effect of substrate on the specific growth rate.

$$\text{Haldane-Andrews model: } \mu = \mu_{\text{max}} \left[\frac{C_{\text{substrate}}}{k_s + C_{\text{substrate}} + \frac{C_{\text{substrate}}^2}{k_{i,s}}} \right] \quad \text{Eq. (3.3)}$$

$$\text{Monod model: } \mu = \mu_{\text{max}} \left[\frac{C_{\text{substrate}}}{k_s + C_{\text{substrate}}} \right] \left(1 - \frac{C_{\text{substrate}}}{C_{\text{substrate}}^*} \right)^n \quad \text{Eq. (3.4)}$$

$$\text{Aiba-Edward model: } \mu = \mu_{\text{max}} \left[\frac{C_{\text{substrate}}}{k_s + C_{\text{substrate}}} \right] e^{-\frac{C_{\text{substrate}}}{k_{i,s}}} \quad \text{Eq. (3.5)}$$

$$\text{Teissier model: } \mu = \mu_{\text{max}} \left(e^{-\frac{C_{\text{substrate}}}{k_{i,s}}} - e^{-\frac{C_{\text{substrate}}}{k_s}} \right) \quad \text{Eq. (3.6)}$$

Where μ is the specific growth rate (1/h)

μ_{max} is the maximum specific growth rate (1/h)

k_s is substrate saturation constant (g-substrate/L)

$k_{i,s}$ is substrate inhibition constant (g-substrate/L)

C_{cell} is cell concentration (g-cell/L)

$C_{\text{substrate}}$ is substrate concentration (g-substrate/L)

$C_{\text{substrate}}^*$ is critical substrate concentration (g-substrate/L)

n is a constant

t is time (h)

The selected models were compared with each other using the coefficient of determination, R^2 , and the variance, σ^2 . The model that had the greatest value of R^2 and the lowest value of σ^2 was selected to be appropriated model.

The coefficient of determination, $R^2 = 1 - \frac{SS_{\text{res}}}{SS_{\text{tot}}}$ **Eq. (3.7)**

Variance, $\sigma^2 = \frac{SS_{\text{tot}}}{df}$ **Eq. (3.8)**

The sum of squares of residuals, $SS_{\text{res}} = \sum_i (y_i - f_i)^2$ **Eq. (3.9)**

The total sum of squares, $SS_{\text{tot}} = \sum_i (y_i - \bar{y})^2$ **Eq. (3.10)**

The mean of the observed data, $\bar{y} = \frac{1}{n} \sum_{i=1}^n y_i$ **Eq. (3.11)**

Where y_i is observed data from experiment

f_i is predicted data from kinetic model

n is number of observed data

df is degree of freedom, number of data – number of model parameters

The account of succinate inhibition of both xylose and glucose fermentation was added to the model of specific growth rate. The critical succinate concentration was evaluated from plotting the relative specific growth rate with the initial succinate concentration. The relative specific growth rate was calculated by the specific growth

rate in the presence of initial succinate concentration divided by the specific growth rate in the absence of initial succinate concentration. At the relative specific growth rate equals zero, the critical succinate concentration was calculated. The expression of succinate inhibition was described as following (Levenspiel, 1980). Moreover, the lysis rate, k_L , was added to represent the cell lysis during the death phase (Rigaki et al., 2020).

$$\mu_{\text{succinate}} = \mu_{\text{max}} \left(1 - \frac{C_{\text{succinate}}}{C_{\text{succinate}}^*} \right)^p \quad \text{Eq. (3.12)}$$

$$k_L = k_{L,\text{max}} \left(\frac{k_1}{C_{\text{substrate}} + k_1} \right) \quad \text{Eq. (3.13)}$$

Where $\mu_{\text{succinate}}$ is specific growth rate on under varying succinate concentrations (1/h)

$C_{\text{succinate}}$ is succinate concentration (g-succinate/L)

$C_{\text{succinate}}^*$ is critical succinate concentration (g-succinate/L)

p is a constant

k_L is lysis rate (1/h)

$k_{L,\text{max}}$ is maximum rate of cell lysis (1/h)

k_1 is lysis constant (g/L)

$C_{\text{substrate}}$ is the substrate concentration (g-substrate/L)

The formation of succinate and acetate were described by Luedking–Piret model.

$\alpha_{\text{succinate}}$ and α_{acetate} are the growth-associated parameters of succinate (g-succinate/g-cell) and acetate productions (g-acetate/g-cell), respectively, and $\beta_{\text{succinate}}$ and β_{acetate} are the non-growth-associated parameters of succinate (g-succinate/g-cell/h) and acetate productions (g-acetate/g-cell/h), respectively.

$$\frac{dC_{\text{succinate}}}{dt} = \alpha_{\text{succinate}} \frac{dC_{\text{cell}}}{dt} + \beta_{\text{succinate}} C_{\text{cell}} \quad \text{Eq. (3.14)}$$

$$\frac{dC_{\text{acetate}}}{dt} = \alpha_{\text{acetate}} \frac{dC_{\text{cell}}}{dt} + \beta_{\text{acetate}} C_{\text{cell}} \quad \text{Eq. (3.15)}$$

Where $C_{\text{succinate}}$ is succinate concentration (g-succinate/L)

C_{acetate} is acetate concentration (g-acetate /L)

Regrading xylose and glucose as substrate, the substrate consumption rate was described *via* combination of equations of product formation and cell growth (Mulchandani et al., 1988) as following.

$$-\frac{dC_{\text{xylose}}}{dt} = \left(\frac{1}{Y_{\text{cell/xylose}}} + \frac{\alpha_{\text{succinate}}}{Y_{\text{succinate/xylose}}} + \frac{\alpha_{\text{acetate}}}{Y_{\text{acetate/xylose}}} \right) \left(\frac{dC_{\text{cell}}}{dt} \right) + \left(\frac{\beta_{\text{succinate}}}{Y_{\text{succinate/xylose}}} + \frac{\beta_{\text{acetate}}}{Y_{\text{acetate/xylose}}} + m_{e,X} \right) C_{\text{cell}} \quad \text{Eq. (3.16)}$$

$$-\frac{dC_{\text{glucose}}}{dt} = \left(\frac{1}{Y_{\text{cell/glucose}}} + \frac{\alpha_{\text{succinate}}}{Y_{\text{succinate/glucose}}} + \frac{\alpha_{\text{acetate}}}{Y_{\text{acetate/glucose}}} \right) \left(\frac{dC_{\text{cell}}}{dt} \right) + \left(\frac{\beta_{\text{succinate}}}{Y_{\text{succinate/glucose}}} + \frac{\beta_{\text{acetate}}}{Y_{\text{acetate/glucose}}} + m_{e,G} \right) C_{\text{cell}} \quad \text{Eq. (3.17)}$$

Where C_{xylose} is xylose concentration (g-xylose/L)

C_{glucose} is glucose concentration (g-glucose/L)

$m_{e,X}$ is cell maintenance coefficient for xylose (g-xylose/L)

$m_{e,G}$ is cell maintenance coefficient for glucose (g-glucose/L)

3.6 The estimation of kinetic parameters

3.6.1 Sensitivity analysis

The relative and absolute parametric sensitivity were initially applied to define the influence and determine the direction of changing initial guess of each parameter (Rigaki et al., 2020). Furthermore, the results were used to define the boundary conditions of each parameters. The normalized sum of squared differences between the experimental and predicted values, function $f(pp)$ (Eq.3.18) was used to demonstrate the effect of each parameter. The 5% of change around its nominal value

of each parameter was conducted, while one parameter was analyzed, the rest parameters were fixed. MATLAB function ode23s was conducted for each set of parameters.

State variables = [C_{cell}, C_{substrate}, C_{succinate}, C_{acetate}]

Parameters, pp = [μ_{\max} , k_s, C_{substrate}^{*}, n, k_I, k_{I,max}, Y_{cell/substrate}, Y_{succinate/substrate},

Y_{acetate/substrate}, m_e, $\alpha_{\text{succinate}}$, α_{acetate} , $\beta_{\text{succinate}}$, β_{acetate} , C_{succinate}^{*}, p]

$$f(\text{pp}) = \sqrt{\left(\sum_{\text{exp}=1}^{\text{nexp}} \sum_{\text{var}=1}^{\text{nvar}} \sum_{\text{p}=1}^{\text{np}} \left(\frac{\hat{y}_{\text{p,exp}} - y_{\text{p,pre}}}{\hat{y}_{\text{p,exp}}} \right)^2 \right)} \quad \text{Eq. (3.18)}$$

$$\text{The absolute parametric sensitivity} = \frac{\Delta f(\text{pp})}{\Delta \text{pp}} \quad \text{Eq. (3.19)}$$

$$\text{The relative parametric sensitivity} = \left| \frac{\Delta f(\text{pp}) \cdot \text{pp}}{\Delta \text{pp} \cdot f(\text{pp})} \right| \quad \text{Eq. (3.20)}$$

Where exp is numbers of experiments, var is numbers of variables, p is numbers of data points, \hat{y} is average of the triplicate experiment, and y is predicted value.

3.6.2 Model calibration

The values of parameters in the proposed mathematic model were estimated based on experimental results from batch fermentations. The initial substrate concentrations at 20, 50, and 80 g/L of xylose and glucose were used to calibrate the parameters via minimization of the function $f(\text{pp})$ (Pateraki et al., 2016). The function $f(\text{pp})$ was conducted using fmincon and ode23s functions in MATLAB to estimate the final optimum set of parameters.

3.6.3 Model validation

The fermentation profiles at initial substrate concentrations of 40 and 60 g/L of xylose and glucose were used to validate the calibrated model. The proficiency

of the kinetic model was estimated using the normalized sum of squared differences between experimental and model predicted results. Model validation was conducted to ensure that the kinetic model could predict the fermentation profiles at comprehensive range of 20-80 g/L from model calibration.



CHAPTER IV

RESULTS AND DISCUSSION

4.1 Fermentation profiles with single substrate

The influence of substrate concentration is not able to be avoided for elaborately studying and understanding process of fermentation. The objective of this experiment was to assess effects of various xylose and glucose concentrations on the cell growth, substrate consumptions, as well as product formations. Those sugars were effectively consumed by *E. coli* KJ12201 under anaerobic conditions. At the beginning, xylose and glucose were separately added in batch fermentation at various concentrations. The concentration of cell, substrates, and products were detected at an appropriated fermentation time interval. The concentrations of xylose and glucose were depicted and discussed in the following sections.

4.1.1 *E. coli* KJ12201 growth

E. coli KJ12201 was individually cultivated with the initial concentration of xylose and glucose in the range of 20-80 g/L (**Figure 4.1** and **4.2**). Within the exponential phase, *E. coli* KJ12201 obviously demonstrated the variant of effective growth with xylose utilization. However, the similarity of growth rate exhibited in glucose as a substrate. After the maximum cell concentration was reached, the death phase of the cell suddenly performed without an evident stationary phase. This phenomenon was illustrated at all initial concentrations of xylose and glucose.

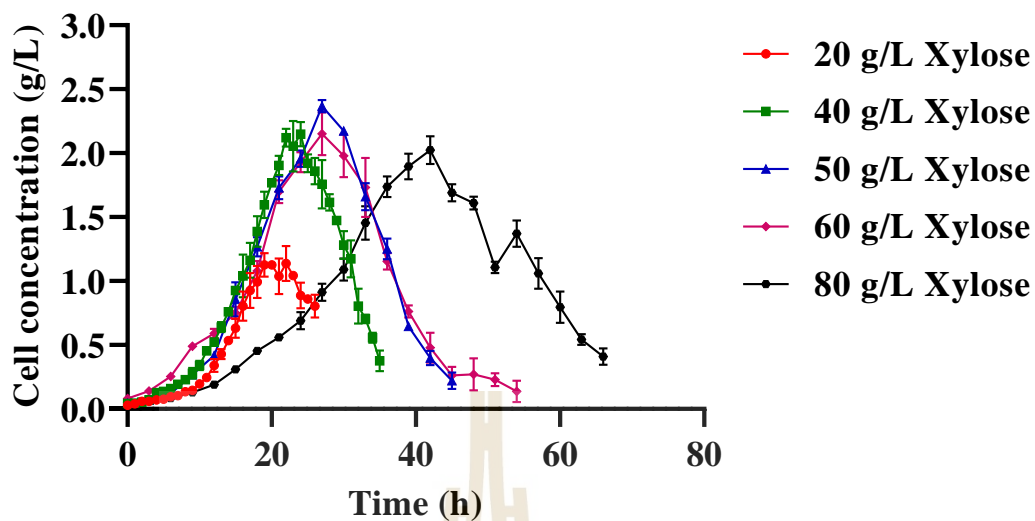


Figure 4.1 The cell concentration profiles of *E. coli* KJ12201 at different initial xylose concentrations.

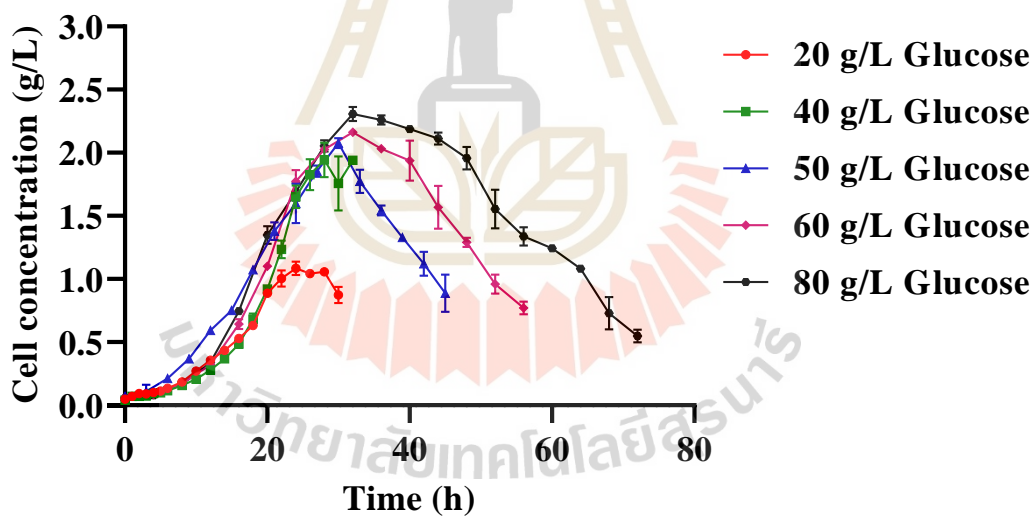


Figure 4.2 The cell concentration profiles of *E. coli* KJ12201 at different initial glucose concentrations.

4.1.2 Substrate consumption

The concentration profiles of xylose and glucose in the fermentation process by *E. coli* KJ12201 were showed in **Figure 4.3** to **4.4**. In pure xylose, it was totally consumed by *E. coli* KJ12201 in ranges of 20-60 g/L. The xylose concentration of 14.71 g/L was approximately remained when the initial xylose concentration 80 g/L was provided (**Figure 4.3**). Therefore, the maximum xylose concentration totally consumed by *E. coli* KJ12201 was around 65.29 g/L. The average consumption rates of xylose were 0.77 ± 0.036 , 1.13 ± 0.012 , 1.13 ± 0.015 , 1.07 ± 0.008 , and 1.01 ± 0.005 g/L/h at the initial xylose concentration of 20, 40, 50, 60, and 80 g/L, respectively. These values were different and rationally related to the growing of *E. coli* KJ12201. At 20 g/L of the initial xylose concentration, results exhibited a high specific growth rate and the highest xylose consumption rate. The xylose consumption rate significantly increased with an increase of initial xylose concentration up to 20 g/L. On the other hands, the xylose consumption rate was reduced at higher initial xylose concentrations greater than 40 g/L. Considering glucose consumption, glucose was totally consumed in overall ranges of 20-80 g/L as in **Figure 4.4**. The glucose consumption rates were 0.73 ± 0.005 , 1.17 ± 0.011 , 1.09 ± 0.014 , 1.10 ± 0.020 , 1.09 ± 0.015 g/L/h at the initial glucose concentrations of 20, 40, 50, 60, and 80 g/L, respectively. These results indicated that the glucose consumption elevated with an increase of initial glucose concentration up to 20 g/L and the similarity of glucose consumption rates was observed within range of 50-80 g/L.

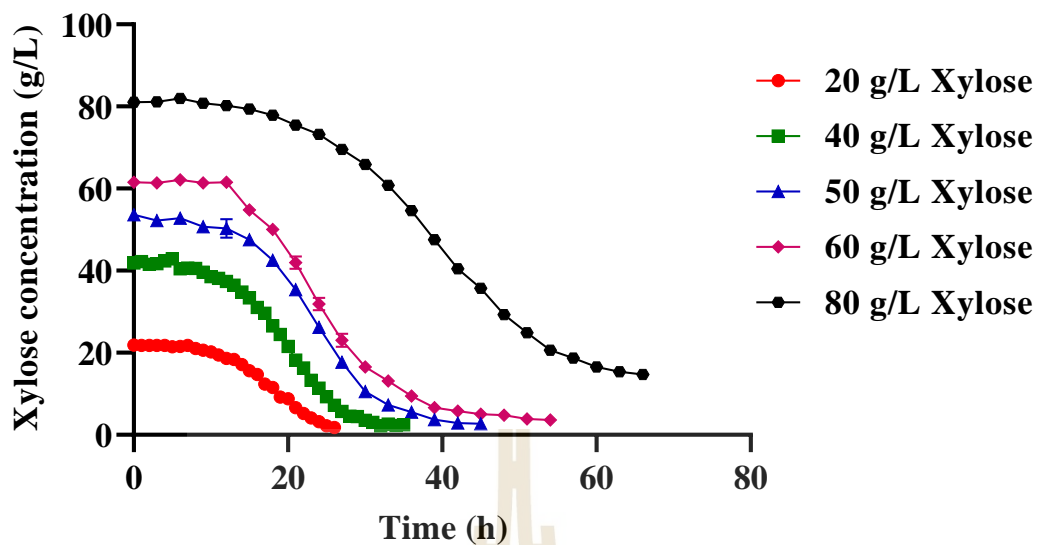


Figure 4.3 The xylose consumption profiles of *E. coli* KJ12201 at different initial xylose concentrations.

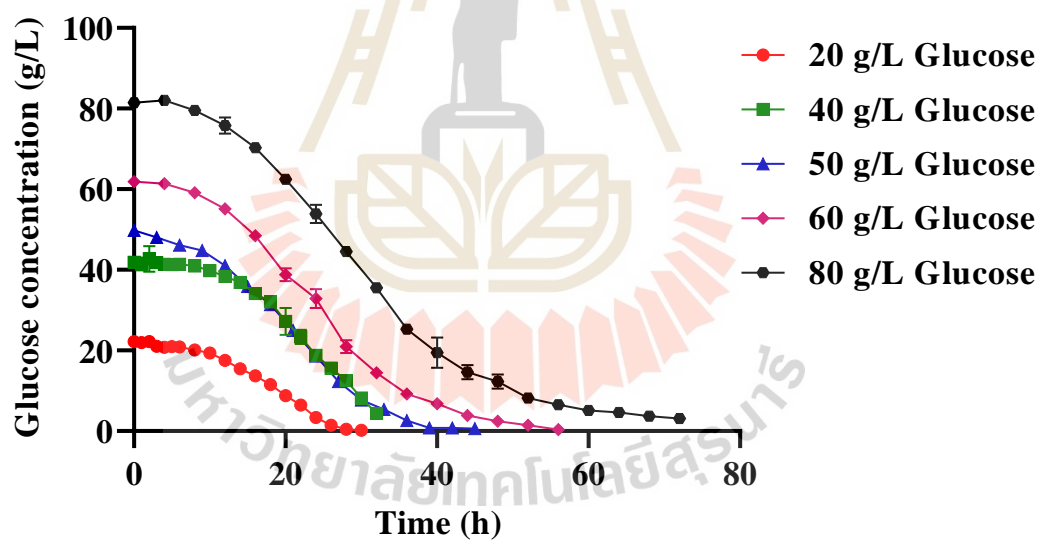


Figure 4.4 The glucose consumption profiles of *E. coli* KJ12201 at different initial glucose concentrations.

4.1.3 Product formation

E. coli KJ12201 produces succinate and acetate as the major products. For the pure xylose substrate, the production profiles of succinate and acetate were shown in **Figure 4.5** and **4.6**, respectively. The production rates were 0.546 ± 0.013 , 0.866 ± 0.022 , 0.856 ± 0.004 , 0.856 ± 0.023 , 0.808 ± 0.043 g/L/h for succinate and 0.096 ± 0.021 , 0.135 ± 0.014 , 0.145 ± 0.005 , 0.136 ± 0.006 , 0.138 ± 0.031 g/L/h for acetate at the initial xylose concentrations of 20, 40, 50, 60, and 80 g/L, respectively. In case of production yield, the succinate yields were 0.707 ± 0.059 , 0.770 ± 0.016 , 0.753 ± 0.013 , 0.835 ± 0.028 , 0.804 ± 0.056 g/g and the acetate yields were 0.140 ± 0.019 , 0.151 ± 0.008 , 0.137 ± 0.006 , 0.148 ± 0.014 , 0.154 ± 0.031 g/g at the initial xylose concentrations of 20, 40, 50, 60, and 80 g/L, respectively. With the range of 20-80 g/L of the initial xylose concentration, the production rate and production yield of succinate and acetate fluctuated.

Regarding glucose utilization, the succinate production profiles and acetate production profiles at various initial glucose concentrations were shown in **Figure 4.7** and **4.8**, respectively. The average production rates were 0.490 ± 0.037 , 0.770 ± 0.020 , 0.848 ± 0.007 , 0.875 ± 0.027 , 0.924 ± 0.008 g/L/h for succinate and 0.065 ± 0.002 , 0.126 ± 0.014 , 0.107 ± 0.005 , 0.096 ± 0.006 , 0.094 ± 0.003 g/L/h for acetate at the initial glucose concentration of 20, 40, 50, 60, and 80 g/L, respectively. Meanwhile, the succinate yields were 0.668 ± 0.009 , 0.657 ± 0.019 , 0.776 ± 0.016 , 0.797 ± 0.014 , 0.850 ± 0.013 g/g and the acetate yields were 0.088 ± 0.004 , 0.108 ± 0.012 , 0.098 ± 0.006 , 0.102 ± 0.007 , 0.090 ± 0.006 g/g at the initial glucose concentrations of 20, 40, 50, 60, and 80 g/L, respectively. The production rate and production yield of succinate

increased with the elevation of initial substrate concentration. However, those of acetate approximately were constant.

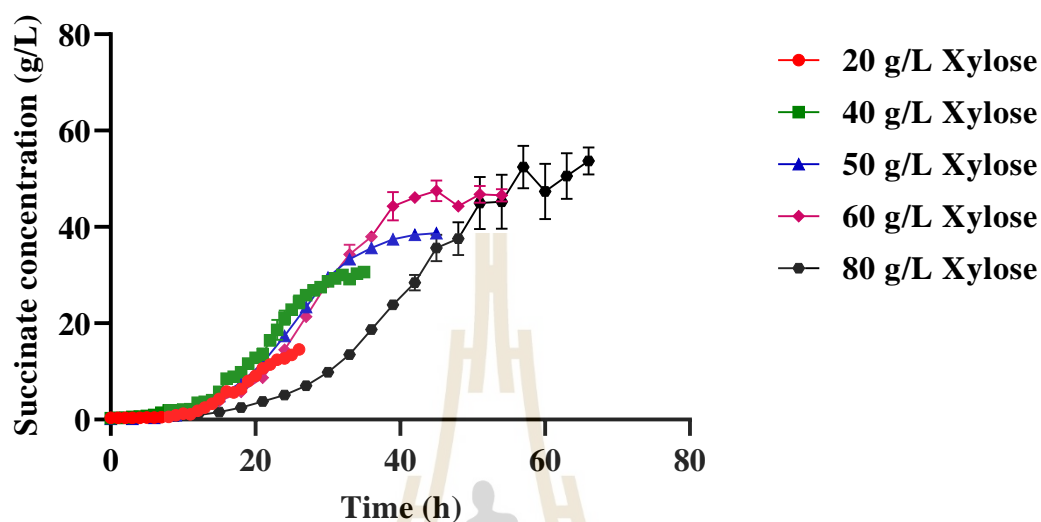


Figure 4.5 The succinate production profiles of *E. coli* KJ12201 at different initial xylose concentrations.

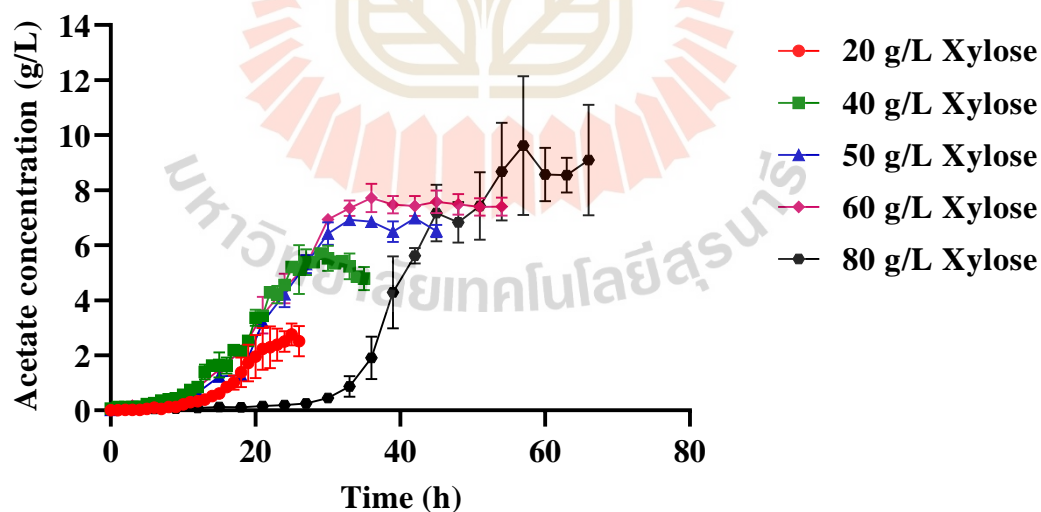


Figure 4.6 The acetate production profiles of *E. coli* KJ12201 at different initial xylose concentrations.

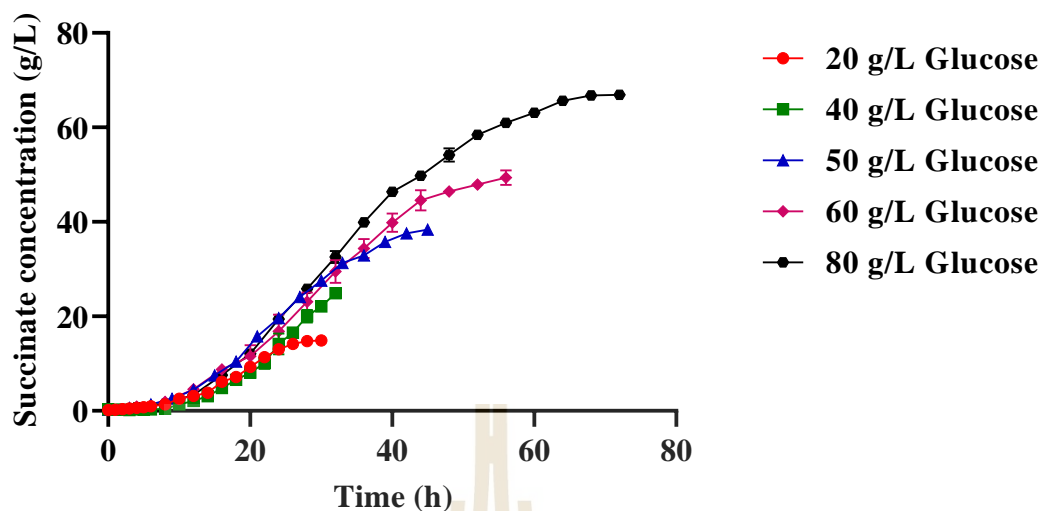


Figure 4.7 The succinate production profiles of *E. coli* KJ12201 at different initial glucose concentrations.

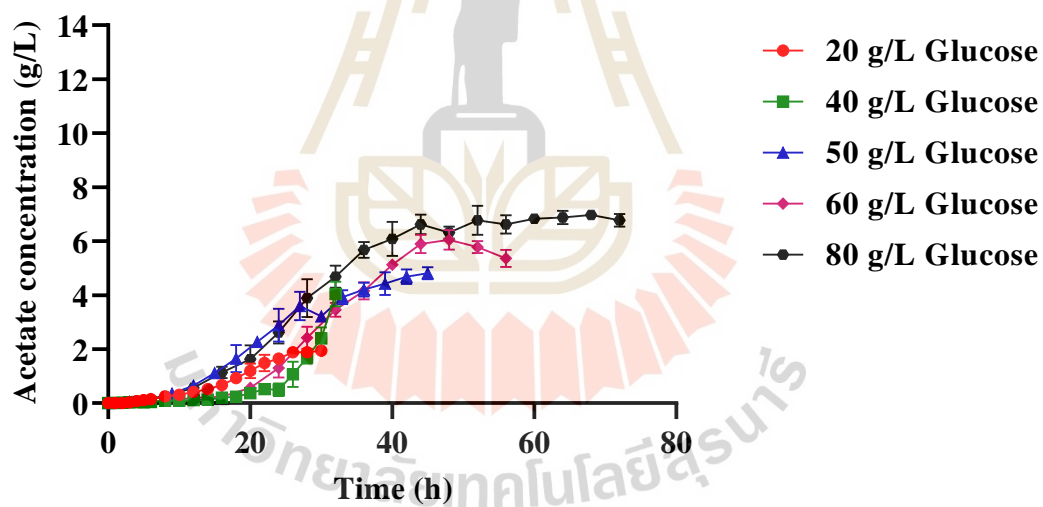


Figure 4.8 The acetate production profiles of *E. coli* KJ12201 at different initial glucose concentrations.

Table 4.1 The summary of fermentation parameters with single substrate.

Initial sugar concentration (g/L)	Yield (g/g)		Productivity (g/h/L)		Termination time of fermentation (h)
	Succinate	Acetate	Succinate	Acetate	
Xylose					
20	0.707±0.059	0.140±0.019	0.546±0.013	0.096±0.021	26
40	0.770±0.016	0.151±0.008	0.866±0.022	0.135±0.014	35
50	0.753±0.013	0.137±0.006	0.856±0.004	0.145±0.005	45
60	0.835±0.028	0.148±0.014	0.856±0.023	0.136±0.006	54
80	0.804±0.056	0.154±0.031	0.808±0.043	0.138±0.031	66
Glucose					
20	0.668±0.009	0.088±0.004	0.490±0.037	0.065±0.002	30
40	0.657±0.019	0.108±0.012	0.770±0.020	0.126±0.014	32
50	0.776±0.016	0.098±0.006	0.848±0.007	0.107±0.005	45
60	0.797±0.014	0.102±0.007	0.875±0.027	0.096±0.006	56
80	0.850±0.013	0.090±0.006	0.924±0.008	0.094±0.003	72

The calculated parameters of the fermentation process with both xylose and glucose as substrates were summarized in **Table 4.1**. The overall succinate yield from utilizing of xylose and glucose were in range of 0.707±0.059 - 0.835±0.028 g/g and 0.657±0.019 - 0.850±0.013 g/g, respectively. The yield and productivity of succinate from xylose were higher than those of glucose at low initial substrate concentrations. Moreover, the higher yield and productivity of acetate were observed from xylose than those of glucose. This supported the improvement efficiency of succinate production

from xylose utilization by *E. coli* KJ12201. Nevertheless, the inhibitory effect at high concentration of xylose significantly influenced the cell growth while glucose had no effect.

4.2 The effect of succinate inhibition

The major product of fermentation by *E. coli* KJ12201 is succinate. The inhibitory concentrations of succinate have been extensively studied to investigate effects on the cell growth of various types of microorganism (Corona-González et al., 2008; Lin et al., 2008; Pateraki et al., 2016; Vlysidis et al., 2011). Therefore, to examine the inhibitory concentration of succinate in the fermentation process by *E. coli* KJ12201, various initial concentrations of succinate were added with the initial sugar concentration of 20 g/L. The initial substrate concentration was appropriately chosen to avoid the side effect from substrate inhibition. The influence of succinate concentration relied on the value of relative specific growth rate. The relationship between the relative specific growth rate and the initial succinate concentration in **Figure 4.9** and **4.10** indicated that the inhibitory concentration of succinate was significantly different between xylose and glucose as carbon substrates. The inhibitory concentration of succinate that completely inhibits the cell growth can be approximated from **Figure 4.9** and **4.10** for xylose and glucose fermentation, respectively.

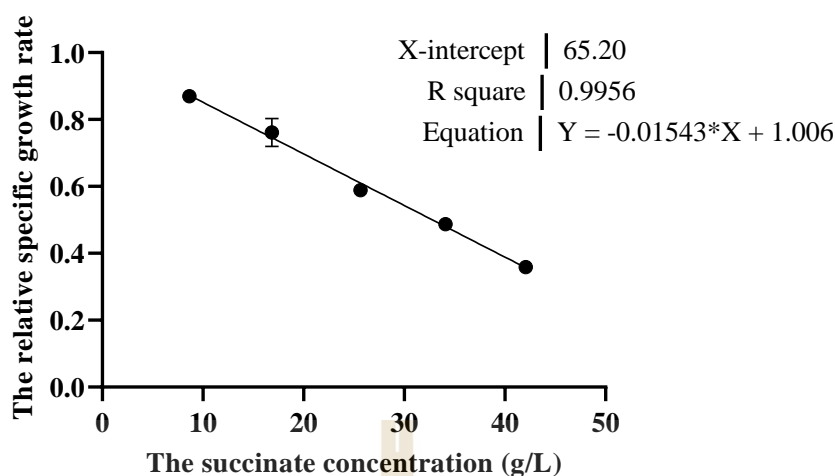


Figure 4.9 The relative specific growth rate of *E. coli* KJ12201 at different initial succinate concentrations of xylose consumption.

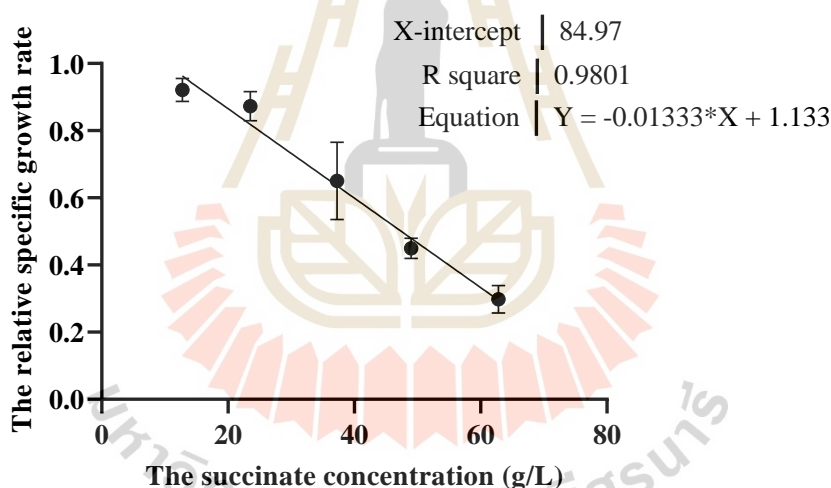


Figure 4.10 The relative specific growth rate of *E. coli* KJ12201 at different initial succinate concentrations of glucose consumption.

Those were 65.20 g/L and 84.97 g/L for the medium containing xylose and glucose, respectively, at the relative specific growth rate of zero. During succinate production, the ATP production is inevitably required for cell maintenance and biomass formation (Varma et al., 1993). The produced ATP from one molecule of glucose and xylose by *E. coli* KJ12201 are 1.8 and 1.67 (Khunnonkwao et al., 2018). Consequently,

E. coli KJ12201 apparently tolerated on the higher concentration of glucose than that of xylose relied on their dissimilarity of cellular energy production.

4.3 Model development

The experimental results from the fermentation process with xylose and glucose consumption by *E. coli* KJ12201 as previous sections were used to calibrate the proposed kinetic model of each substrate through parameter estimation. The initial substrate concentration of 20, 50, and 80 g/L were used for calibrating the kinetic model. Afterward, at initial substrate concentration of 40 and 60 g/L were used for validating the kinetic model. The yields of cell mass ($Y_{\text{cell/xylose}}$ and $Y_{\text{cell/glucose}}$), succinate ($Y_{\text{succinate/xylose}}$ and $Y_{\text{succinate/glucose}}$), and acetate ($Y_{\text{acetate/xylose}}$ and $Y_{\text{acetate/glucose}}$) proposed in the equation were assumed to be identical for all experiments. The appropriated specific growth rate model was selected from Haldane-Andrews, Monod, Aiba-Edward, and Teissier models. The inhibitory effect of succinate concentration was separately applied in an equation of the cell growth rate limitation with xylose and glucose consumptions. The influence of each parameter was analyzed by the relative parametric sensitivity and absolute parametric sensitivity (Rigaki et al., 2020). The initial guesses for parameter estimations were taken from experimental results.

4.3.1 The specific growth rate model

The specific growth rate was calculated from slope via plotting \ln (cell concentration) versus fermentation time within an exponential phase (results not shown). The values of specific growth rates with xylose and glucose at various concentrations were shown in **Figure 4.11** and **4.12**. The specific growth rate rapidly raised up with an increase in initial xylose concentration up to 20 g/L. Nevertheless, of the initial xylose concentration greater than 20 g/L, it indicated the beginning of cell

growth inhibition. Meanwhile, the specific growth rate with an increase in initial glucose concentration suddenly elevated and was not hindered by the substrate inhibition. Therefore, the specific growth rate model for only xylose consumption was described using model of Haldane- Andrews, Monod, Aiba- Edward, or Teissier. Meanwhile, kinetic model for glucose was Monod model.

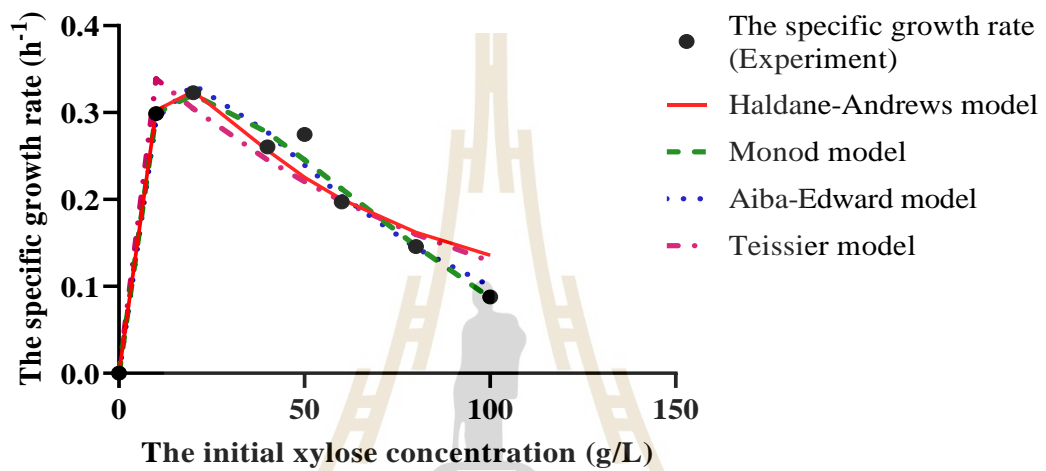


Figure 4.11 The specific growth rate of *E. coli* KJ12201 at different initial xylose concentrations.

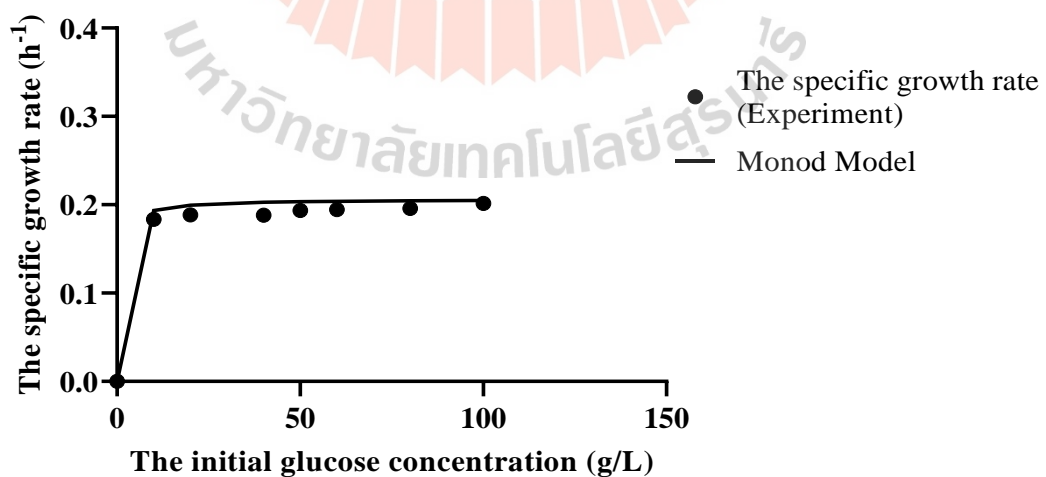


Figure 4.12 The specific growth rate of *E. coli* KJ12201 at different initial glucose concentrations.

The comparison between experimental results with model prediction of xylose and glucose was shown in **Figure 4.11** and **4.12**. Parameters of the proposed model were evaluated by nonlinear curve-fitting with values of the specific growth rate at various initial substrate concentrations from experiments. Statistical measures indicated the precision of model prediction to experimental results. The estimated parameters and statistical measures were summarized in **Table 4.2**. Smallest variance, σ^2 and greatest coefficient of determination, R^2 predicted the better model compared to the other models. Using xylose as a substrate, the Monod model offered the lowest variance ($\sigma^2 = 0.000342$) with the acceptable coefficient of determination ($R^2 = 0.985$). Consequently, the Monod model may be a suitable predicting model for xylose fermentation. Previous studies reported that the Monod model was the appropriated model for predicting specific growth rate with substrate inhibition account (Kim et al., 2016; Luong, 1987). Based on the Monod model, estimate values of μ_{\max} , k_s , $C^*_{\text{substrate}}$ and n for xylose were 0.495 1/h, 4.94 g/L, 143.5 g/L, and 1.42, respectively. When glucose was used as substrate, the Monod model demonstrated the better prediction with a higher coefficient of determination ($R^2 = 0.998$) and low variance ($\sigma^2 = 0.000010$) in which estimated values of μ_{\max} and k_s were 0.198 1/h and 0.87 g/L. The maximum growth rate of xylose fermentation ($\mu_{\max} = 0.495$ 1/h) was higher than that of glucose ($\mu_{\max} = 0.198$ 1/h). These estimated values indicated that the cell growth of *E. coli* KJ12201 apparently preferred xylose utilization. However, the influence of substrate inhibition affected the specific growth rate at high initial xylose concentration. Consequently, the specific growth rate in xylose obviously reduced with an increase in initial concentration. The Monod constant (k_s) of xylose (4.94 g/L) and glucose (0.87 g/L) demonstrated the dissimilarity of substrate affinity. These values presumably indicated that the maximum specific growth rate in glucose utilization was reached at lower initial concentration than that of xylose as **Figure 4.11** and **4.12**.

Table 4.2 Estimated parameters and statistic measures obtained from various models.

Substrate	Model	Estimated parameters							Statistic measures			
		μ_{max}	K_s	$k_{i,s}$	$C^*_{substrate}$	n	Min	Max	Squared norm of the residual	Degree of freedom, df	σ^2	R^2
Xylose	Haldane-Andrews	1.000	16.86	16.14	-	-	-0.0493	0.0481	0.00505	5	0.001009	0.944
	Monod	0.495	4.94	-	143.5	1.42	-0.0294	0.0166	0.00137	4	0.000342	0.985
	Aiba-Edward	0.784	12.03	51.53	-	-	-0.0352	0.0168	0.00186	5	0.000371	0.979
	Teissier	0.377	0.10	93.20	-	-	-0.0542	0.0413	0.00699	5	0.001399	0.922
Glucose	Monod	0.198	0.87	-	-	-	-0.0056	0.0052	0.00006	6	0.000010	0.998

Finally, the specific growth rate of xylose (subscript X) and glucose (subscript G) consumptions were described as the following equations.

$$\mu_X = (0.495 \text{ 1/h}) \left(\frac{C_{\text{xylose}}}{C_{\text{xylose}} + 4.94 \text{ g/L}} \right) \left(1 - \frac{C_{\text{xylose}}}{143.5 \text{ g/L}} \right)^{1.42} \quad \text{Eq.(4.1)}$$

$$\mu_G = (0.198 \text{ 1/h}) \left(\frac{C_{\text{glucose}}}{C_{\text{glucose}} + 0.87 \text{ g/L}} \right) \quad \text{Eq.(4.2)}$$

Regarding the maximum specific growth rate of different microbial types for producing succinate, previous studies widely investigated the kinetic growth rate with various substrates. The estimated parameters that were proposed in the specific growth rate model of each succinate producer was summarized in **Table 4.3**. Using xylose-based substrate, the growth rate analysis using the Haldane-Andrews model of *Actinobacillus succinogenes* 103Z and *Basfia succiniciproducens* JF4016 was applied (Pateraki et al., 2016). Results demonstrated that the maximum specific growth rate of *E. coli* KJ12201 ($\mu_{\text{max}} = 0.495 \text{ 1/h}$) was greater than that of *A. succinogenes* 130Z ($\mu_{\text{max}} = 0.39 \text{ 1/h}$) except *B. succiniciproducens* JF4016 ($\mu_{\text{max}} = 0.93 \text{ 1/h}$). However, a higher value of maximum specific growth rate ($\mu_{\text{max}} = 0.93 \text{ 1/h}$) of *B. succiniciproducens* JF4016 could be a result of the use of a mixed substrate including 72.6% xylose with 12.2% galactose, 10.9% glucose, 4.2% mannose, and 0.1% arabinose. Additionally, the growth rate of *E. coli* KJ12201 (at which $k_s = 4.94 \text{ g/L}$) was achieved at higher xylose concentration than those of *A. succinogenes* 130Z (at which $k_s = 0.698 \text{ g/L}$) and *B. succiniciproducens* JF4016 (at which $k_s = 1.56 \text{ g/L}$).

Table 4.3 The parameters of specific growth rate model of each succinate producer.

Substrate	Microorganism	Model	Estimated parameters				Reference
			μ_{\max}	k_s	$k_{i,s}$	$C^*_{\text{substrate}}$	
Xylose	<i>Actinobacillus succinogenes</i> 103Z	Haldane-Andrews	0.39	0.698	55.48	-	Pateraki et al., 2016
	<i>Basfia succiniciproducens</i> JF4016	Haldane-Andrews	0.93	1.56	15.17	-	Pateraki et al., 2016
	<i>Escherichia coli</i> KJ12201	Monod	0.495	4.94	-	143.5	This study
Glucose	<i>Actinobacillus succinogenes</i> (ATCC 55618)	Extended Monod	0.50	2.03	-	155	Lin et al., 2008
	<i>Actinobacillus succinogenes</i> 130Z	Haldane-Andrews	0.40	2.8	78.7	-	Luthfi et al., 2018
	<i>Escherichia coli</i> KJ12201	Monod	0.198	0.87	-	-	This study

For glucose fermentation under anaerobic conditions, the maximum specific growth rate of *Actinobacillus succinogenes* (ATCC 55618) and *Actinobacillus succinogenes* 130Z were 0.5 1/h (Lin et al., 2008) and 0.4 1/h (Luthfi et al., 2018) evaluated using an extended Monod and Haldane models, respectively. This showed the lower growth rate in glucose fermentation of *E. coli* KJ12201 ($\mu_{\max} = 0.198$ 1/h) compared to *A. succinogenes* (ATCC 55618 and 130Z). However, the glucose tolerance of *E. coli* KJ12201 considerably greater than those of *A. succinogenes* (ATCC 55618 and 130Z). The glucose inhibition thus affecting to cell growth rates of *A. succinogenes* ATCC 55618 ($C^*_{\text{Glucose}} = 155$ g/L) and *A. succinogenes* 130Z ($k_{i,s} = 78.7$ g/L) (Lin et al., 2008; Luthfi et al., 2018) began at the glucose concentration above 40 g/L while *E. coli* KJ12201 was not yet affected.

4.3.2 Sensitivity analysis

The sensitivity analysis was applied for the proposed model parameters in xylose and glucose. The 16 parameters for model prediction in xylose were μ_{\max} , k_s , C_{xylose}^* , n , $k_{l,\max}$, k_l , $Y_{\text{cell/xylose}}$, $Y_{\text{succinate/xylose}}$, $Y_{\text{acetate/xylose}}$, m_e , $\alpha_{\text{succinate}}$, α_{acetate} , $\beta_{\text{succinate}}$, β_{acetate} , $C_{\text{succinate}}^*$, and p . The 14 parameters for model prediction in glucose were μ_{\max} , k_s , $k_{l,\max}$, k_l , $Y_{\text{cell/glucose}}$, $Y_{\text{succinate/glucose}}$, $Y_{\text{acetate/glucose}}$, m_e , $\alpha_{\text{succinate}}$, α_{acetate} , $\beta_{\text{succinate}}$, β_{acetate} , $C_{\text{succinate}}^*$, and p . The function $f(pp)$ was used to identify the sensitive parameters via relative parametric sensitivity equation. Moreover, the direction of function $f(pp)$ value on each parameter was analyzed by the absolute parametric sensitivity. The percent change of function $f(pp)$, relative parametric sensitivity, and absolute parametric sensitivity were showed as following. The changes of each parameter value with 5% increase and decrease influenced the solution of function $f(pp)$ as in **Figure 4.13** and **4.14** for xylose and glucose, respectively. The relative and absolute parametric sensitivity for xylose and glucose were summarized in **Table 4.4** and **4.5**, respectively. The relative parametric sensitivity indicated the sensitive parameters as compared to each other. For instance, the highest relative parametric sensitivity of C_{xylose}^* and μ_{\max} indicated their extreme influence on the solution of function $f(pp)$ compared to others for xylose and for glucose, respectively. The direction of changing parameter value was also analyzed via absolute parametric sensitivity. For instance, a decrease of k_s elevated the value of function $f(pp)$ for both xylose and glucose.

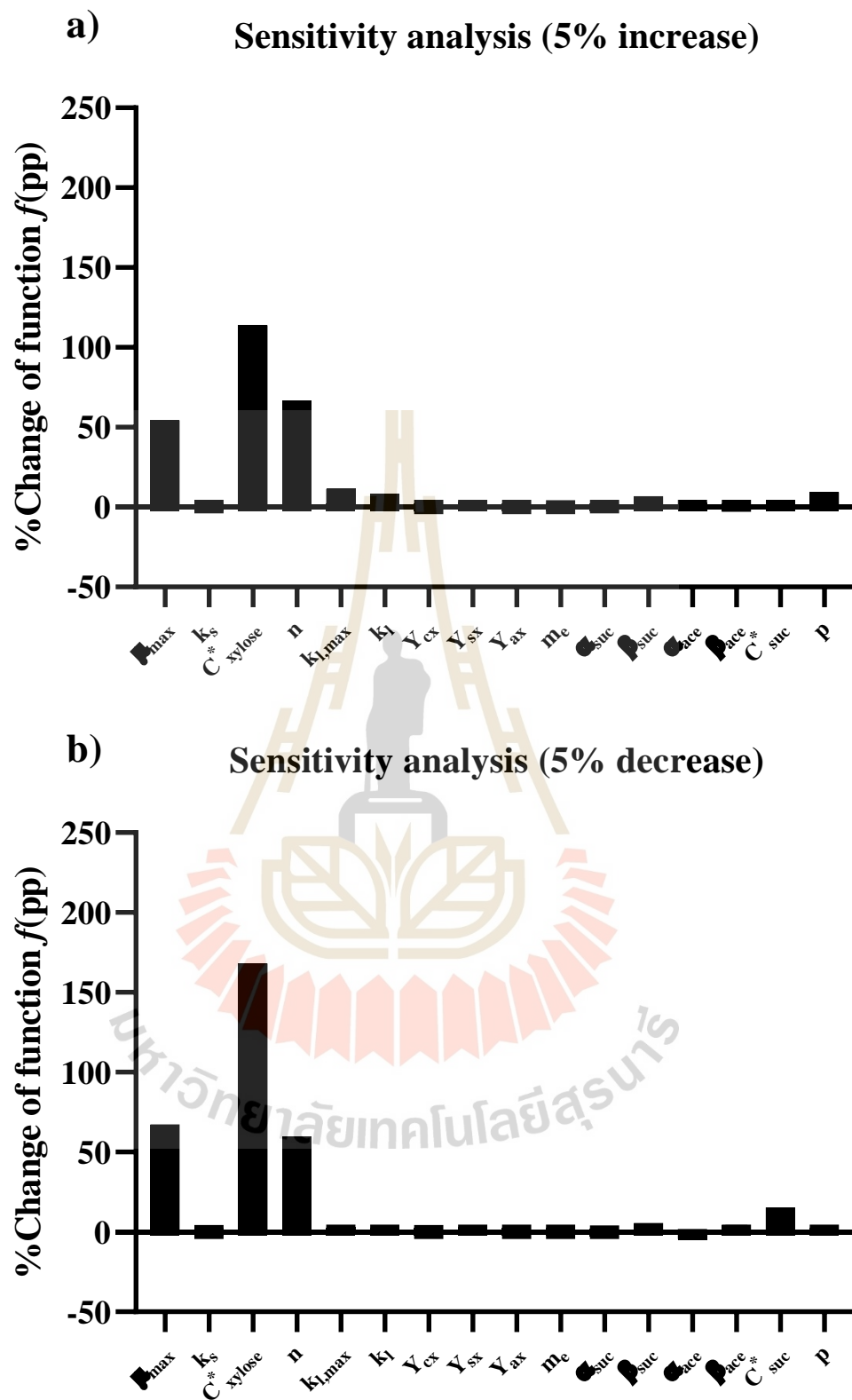


Figure 4.13 The relationship between %change of function $f(pp)$ on (a) 5% increase and (b) decrease of each parameter value in model prediction of xylose.

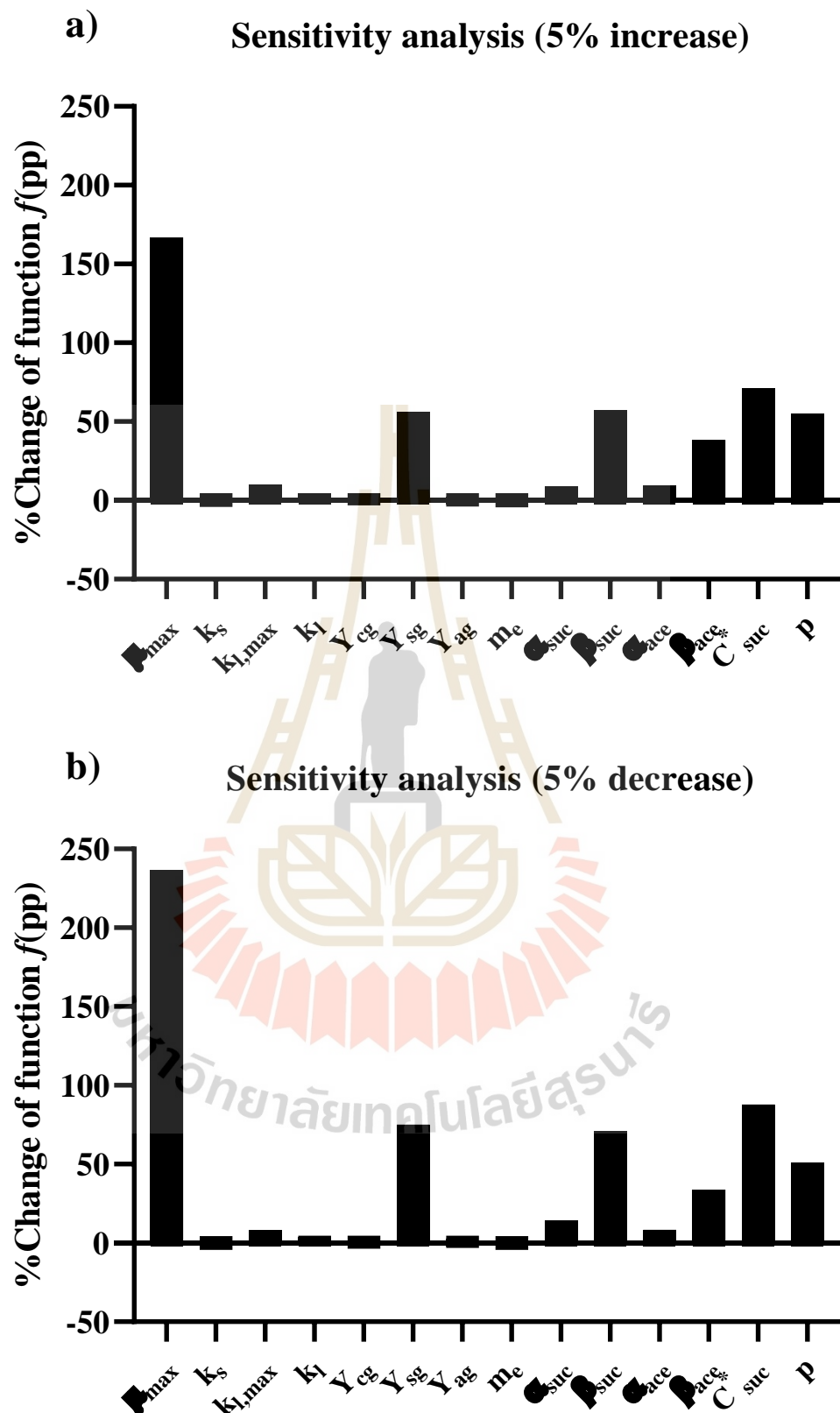


Figure 4.14 The relationship between %change of function $f(pp)$ on (a) 5% increase and (b) decrease of each parameter value in model prediction of glucose.

Table 4.4 The relative and absolute parametric sensitivity for model prediction of xylose.

Parameter	5% Increase		5% Decrease	
	Absolute sensitivity	Relative sensitivity	Absolute sensitivity	Relative sensitivity
μ_{\max}	16.709	11.121	-19.888	13.237
k_s	0.019	0.129	0.003	0.023
C^*_{xylose}	0.118	22.769	-0.174	33.620
n	6.933	13.231	-6.260	11.946
$k_{l,\max}$	3.900	1.867	-1.816	0.869
k_l	0.134	1.702	-0.040	0.510
$Y_{\text{cell/xylose}}$	0.010	0.009	0.006	0.006
$Y_{\text{succinate/xylose}}$	0.517	0.667	-0.487	0.628
$Y_{\text{acetate/xylose}}$	0.036	0.043	-0.008	0.010
m_e	-2.318	0.016	-0.032	0.000
$\alpha_{\text{succinate}}$	0.041	0.124	0.022	0.064
$\beta_{\text{succinate}}$	1.157	1.343	-0.992	1.150
α_{acetate}	0.435	0.589	0.369	0.500
β_{acetate}	1.682	0.315	-4.543	0.849
$C^*_{\text{succinate}}$	0.010	0.901	-0.034	3.076
p	0.602	1.833	-0.196	0.596

Table 4.5 The relative and absolute parametric sensitivity for model prediction of glucose.

Parameter	5% Increase		5% Decrease	
	Absolute sensitivity	Relative sensitivity	Absolute sensitivity	Relative sensitivity
μ_{\max}	10.643	33.375	-15.086	47.306
k_s	0.004	0.060	0.003	0.046
$k_{l,\max}$	1.513	1.988	-1.237	1.626
k_l	0.007	0.925	-0.006	0.752
$Y_{\text{cell/glucose}}$	0.075	0.280	-0.053	0.196
$Y_{\text{succinate/glucose}}$	0.717	11.241	-0.959	15.033
$Y_{\text{acetate/glucose}}$	0.010	0.141	-0.021	0.299
m_e	0.072	0.005	0.062	0.004
$\alpha_{\text{succinate}}$	0.022	1.734	-0.037	2.844
$\beta_{\text{succinate}}$	1.049	11.466	-1.299	14.197
α_{acetate}	0.097	1.893	-0.085	1.653
β_{acetate}	7.324	7.655	-6.471	6.764
$C^*_{\text{succinate}}$	0.011	14.188	-0.014	17.571
p	0.189	10.978	-0.176	10.209

4.3.3 Model calibration

Estimated values of parameters were summarized as in **Table 4.6**. The growth-associated parameter ($\alpha_{\text{succinate}}$) and non-growth associated parameter ($\beta_{\text{succinate}}$) implied the efficiency of succinate production within the period of exponential and stationary phase, respectively. The production of succinate was obviously produced within exponential phase ($\alpha_{\text{succinate}} = 2.22$ g-succinate/g-cell for xylose and $\alpha_{\text{succinate}} = 4.91$ g-succinate/g-cell for glucose). Meanwhile, within stationary phase, smaller amounts of succinate concentration were produced ($\beta_{\text{succinate}} = 0.86$ g-succinate/g-cell/h for xylose and $\beta_{\text{succinate}} = 0.69$ g-succinate/g-cell/h for glucose). Unsurprisingly, succinate is a growth associated metabolite.

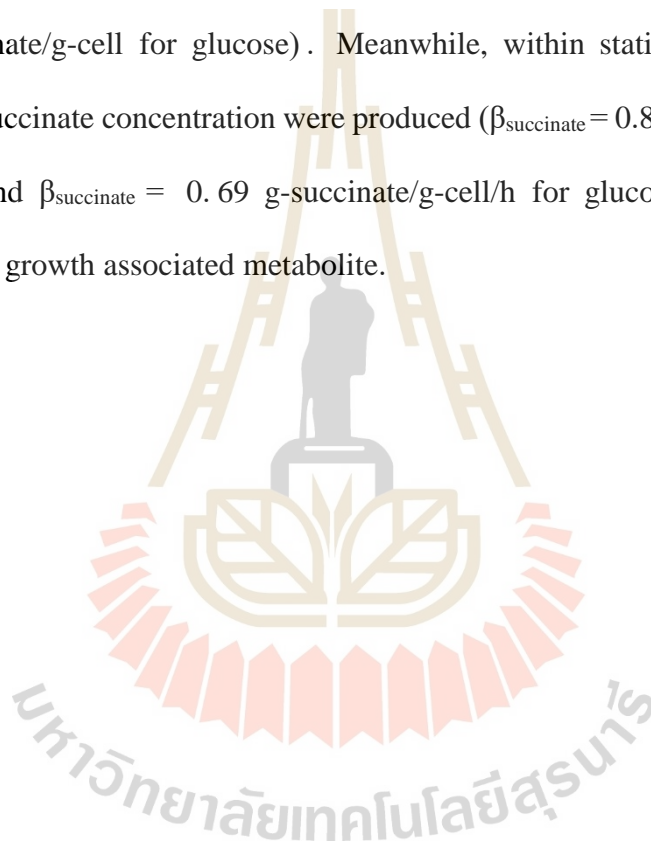


Table 4.6 Estimated values of parameters for the fermentation process by *E. coli* KJ12201 with various initial concentrations of xylose and glucose.

Parameter	Description	Units	Substrate	
			Xylose	Glucose
μ_{\max}	Maximum specific growth rate	1/h	0.495	0.198
k_s	Substrate saturation constant	g/L	4.94	0.87
$C^*_{\text{substrate}}$	Critical substrate concentration	g/L	143.5	-
n	Power constant for substrate inhibition	-	1.42	-
$k_{l,\max}$	Maximum rate of cell lysis	1/h	0.36	0.08
k_l	Cell lysis constant	g/L	9.42	8.12
$Y_{\text{cell,substrate}}$	Yield of cell to substrate	g-cell/g-substrate	0.721	0.235
$Y_{\text{succinate,substrate}}$	Yield of succinate to substrate	g-succinate/g-substrate	0.960	0.990
$Y_{\text{acetate,substrate}}$	Yield of acetate to substrate	g-acetate/g-substrate	0.879	0.899
m_e	Maintenance coefficient	g-substrate/g-cell/h	0.005	0.004
$\alpha_{\text{succinate}}$	Growth associated constant for succinate	g-succinate/g-cell	2.22	4.91
$\beta_{\text{succinate}}$	Non-growth associated constant for succinate	g-succinate/g-cell/h	0.86	0.69
α_{acetate}	Growth associated constant for acetate	g-acetate/g-cell	1.01	1.23
β_{acetate}	Non-growth associated constant for acetate	g-acetate/g-cell/h	0.14	0.07
$C^*_{\text{succinate}}$	Critical succinate concentration	g-succinate/L	68.19	81.48
p	Power constant for succinate inhibition	-	2.27	3.66

Considering the succinate yield, *E. coli* KJ12201 was considerably the effective succinate producer in fermentation process from xylose as substrate. The succinate yield from xylose fermentation estimated by the proposed model was 0.960 g/g. This was acceptable value compared with that of 0.87 g/g based on the previous experiment data (Khunnonkwao et al., 2018). The previous studies reported estimated parameters in the kinetic models of several succinate producers. The produced succinate from xylose within an exponential phase of *E. coli* KJ12201 ($\alpha_{\text{succinate}} = 2.22$ g-succinate/g-cell) was lower than that of *A. succinogenes* ($\alpha_{\text{succinate}} = 3.86$ g-succinate/g-cell) and *B. succiniciproducens* ($\alpha_{\text{succinate}} = 4.08$ g-succinate/g-cell) (Pateraki et al., 2016). Regarding the glucose fermentation, *E. coli* KJ12201 promisingly produced amount of succinate ($\alpha_{\text{succinate}} = 4.91$ g-succinate/g-cell) during the exponential phase at a higher level than that of *A. succinogenes* ATCC 55618 ($\alpha_{\text{succinate}} = 3.60$ g-succinate/g-cell). Additionally, acetate concentration was produced with a small concentration during both exponential and stationary phases ($\alpha_{\text{acetate}} = 1.01$ g-succinate/g-cell, $\beta_{\text{acetate}} = 0.14$ g-succinate/g-cell/h for xylose and $\alpha_{\text{acetate}} = 1.23$ g-succinate/g-cell, $\beta_{\text{acetate}} = 0.07$ g-succinate/g-cell/h for glucose). These estimated values demonstrated that *E. coli* KJ12201 seldom produced by-products.

The inhibition of succinate concentration to growth of *E. coli* had been reported in previous studies. Of 80 g/L succinate concentration in glucose fermentation completely inhibited the growth of *E. coli* stain NZN111, AFP111, and BL21 (Li et al., 2010). This value was similar to the maximum inhibiting succinate concentration of *E. coli* KJ12201 ($C^*_{\text{succinate}} = 81.48$ g/L). Concerning comparison with other succinate producers, *E. coli* KJ12201 performed the greatest tolerance in glucose fermentation compared to *Actinobacillus succinogenes* ATC 55618 ($C^*_{\text{succinate}} = 45.6$ g/L) (Lin et al.,

2008). Using xylose as substrate, *E. coli* KJ12201 ($C^*_{\text{succinate}} = 68.19 \text{ g/L}$) was completely inhibited at the higher succinate concentration than 55 g/L compared to those of both *Actinobacillus succinogenes* 130Z and *Basfia succiniciproducens* JF4016 (Pateraki et al., 2016).

The model predictions of cell concentration, substrate consumption, and product formation with various initial substrate concentrations were in an agreement with the experiment results as illustrated in **Figure 4.15**. The comparison between experimental data and model prediction was assessed via the normalized sum of squared differences in **Table 4.7**. The range of the normalized sum of squared differences for model prediction of xylose and glucose were 0.095-53.50 and 0.019-15.13, respectively.

Table 4.7 The normalized sum of squared differences between experimental data and model prediction of model calibration.

The normalized sum of squared differences				
Concentration (g/L)	Cell growth	Substrate	Succinate	Acetate
Xylose				
20	0.095	6.030	4.591	1.843
50	0.117	5.103	1.078	1.600
80	0.315	4.520	53.50	24.75
Glucose				
20	0.019	1.881	4.532	0.034
50	0.067	6.314	2.846	0.957
80	0.107	15.13	4.510	1.459

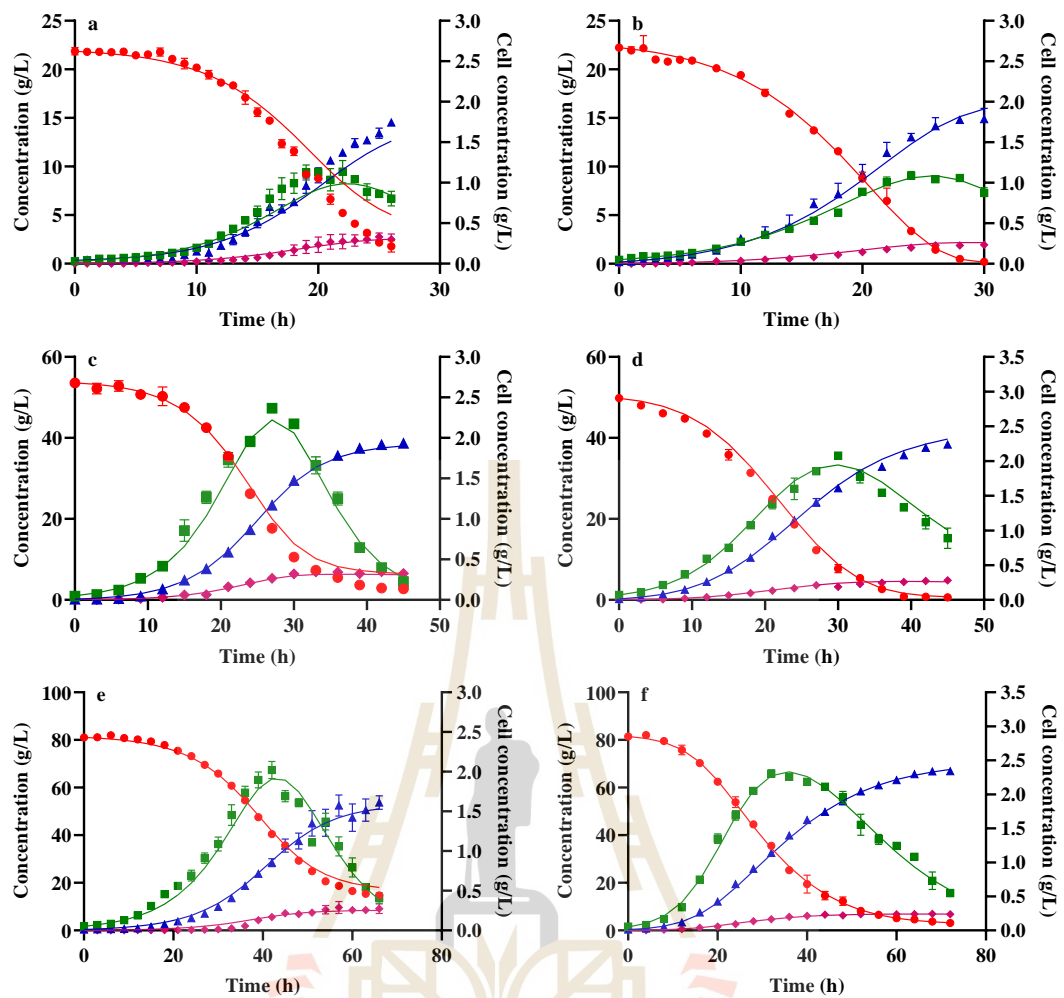


Figure 4.15 The experimental and model predicted profiles at initial substrate concentration of model calibration. Left and right panels for xylose and glucose, respectively. **a-b** 20 g/L, **c-d** 50 g/L, and **e-f** 80 g/L. Symbols: cell concentration (green square), xylose concentration (red circle), succinate concentration (blue triangle), and acetate concentration (magenta diamond).

4.3.4 Model validation

The kinetic model was used to estimate the fermentation profiles of succinate production by *E. coli* KJ12201 under anaerobic conditions using 40 and 60 g/L of individual xylose and glucose. The comparison between experimental and model predicted profiles of xylose and glucose were showed as **Figure 4.16**. The normalized sum of squared differences between experiments and model predictions of concentration of cell, substrate, succinate, and acetate were summarized in **Table 4.8**.

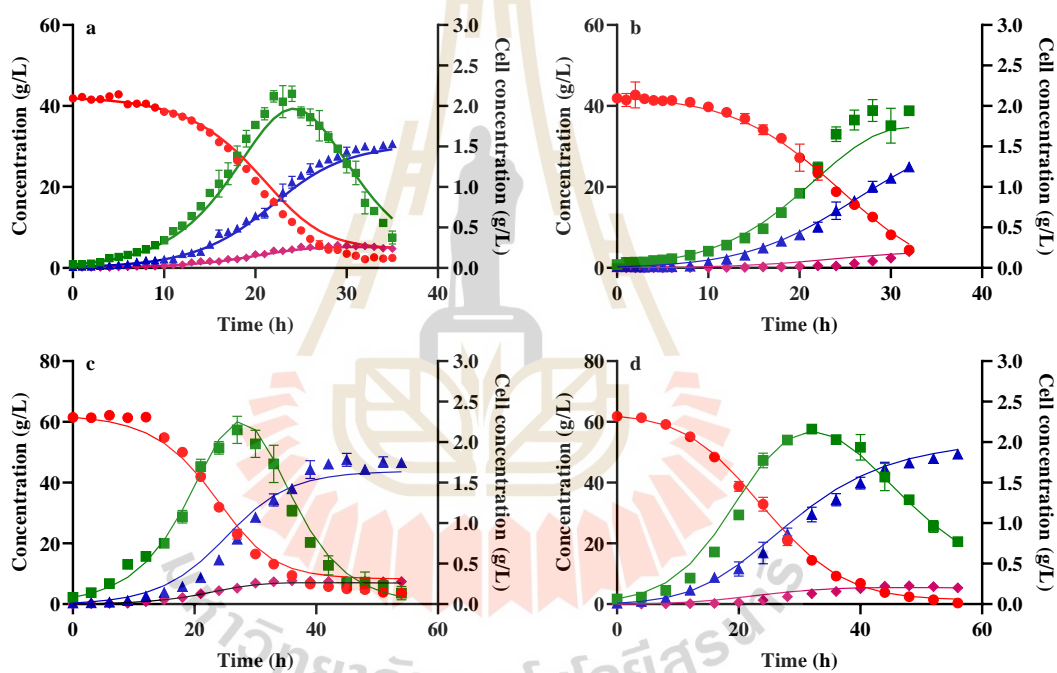
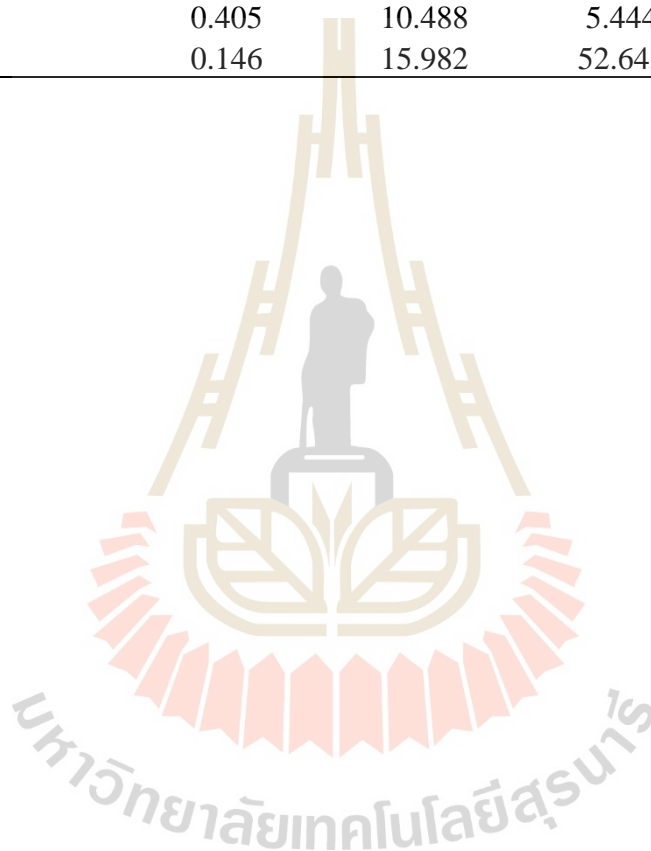


Figure 4.16 The experimental and model predicted profiles at initial substrate concentration of model validation. Left and right panels for xylose and glucose, respectively. **a-b** 40 g/L and **c-d** 60 g/L. Symbols: cell concentration (green square), xylose concentration (red circle), succinate concentration (blue triangle), and acetate concentration (magenta diamond).

Table 4.8 The normalized sum of squared differences between experimental data and model prediction of model validation.

Concentration (g/L)	The normalized sum of squared differences			
	Cell growth	Substrate	Succinate	Acetate
Xylose				
40	0.937	9.740	0.319	0.519
60	0.752	5.129	4.797	0.859
Glucose				
40	0.405	10.488	5.444	13.445
60	0.146	15.982	52.643	12.749



CHAPTER V

SUMMARY AND FUTURE PLAN

5.1 Summary

This study focused on evaluating the inhibitory effect of substrate and product and applying the kinetic models with experimental data from the fermentation process for succinate production by *E. coli* KJ12201. *E. coli* KJ12201 was genetically modified to improve the succinate production from glucose and xylose. Therefore, xylose and glucose were separately used as a single substrate for cultivating this strain in this study. The fermentation profiles depicted the effectiveness of succinate production from xylose after the strain development by metabolic engineering. Based on the experimental data, the maximum yield of succinate was 0.835 ± 0.028 g/g for xylose and 0.850 ± 0.013 g/g for glucose. Concerning substrate inhibition, xylose apparently exhibited an inhibitory effect on cell growth at the concentration higher than 20 g/L. Meanwhile, the inhibition of cell growth by glucose in ranges of 20-80 g/L was not observed. From results of substrate inhibition, the inhibition of glucose was negligible but not for xylose. Haldane-Andrews, Monod model, Aiba-Edward, or Teissier models were used to express the specific growth rate for xylose while the Monod model was used for glucose. The Monod model precisely predicted the specific growth rate for utilizing xylose with the lowest variance ($\sigma^2 = 0.000342$) and the acceptable coefficient of determination ($R^2 = 0.985$). The Monod model demonstrated the acceptable prediction for glucose with low variance ($\sigma^2 = 0.000010$) and high coefficient of determination ($R^2 = 0.998$). Based on the succinate inhibition from kinetic model,

it indicated the maximum succinate concentration that completely inhibited the cell growth was 81.48 g/L when glucose was used as a substrate. This was higher than the maximum succinate concentration of 68.19 g/L in xylose containing medium. These results relied on the hypothesis of ATP production. *E. coli* KJ12201 produced the net ATP from one molecule of glucose higher than that of xylose. The higher ATP could be effectively used for the cell growth and maintenance. Therefore, the tolerance of *E. coli* KJ12201 on succinate concentration was also elevated as observed in the medium containing glucose than that of xylose. The combination term of substrate and product inhibitions was additionally used to predict the concentration of cell, substrate utilization, and product formation at various initial concentrations of xylose and glucose. The comparison between experimental data and model prediction of model calibration depicted the capability of kinetic model with a reasonable and acceptable normalized sum of squared differences. Moreover, the kinetic model was validated with another set of experimental data and the model prediction was in good agreement with experimental data. This indicated that the proposed model provided reasonable prediction of the behavior of the succinate fermentation process using xylose and glucose as a substrate.

5.2 Future plan

The optimization of kinetic model will helpfully define the optimum condition for interested parameters. Since lignocellulosic biomass mainly contains xylose and glucose, a development of kinetic model for mixed xylose/glucose is a promising step to demonstrate the proficiency of *E. coli* KJ12201 on lignocellulosic biomass as a substrate.

REFERENCES

- Aiba, S., Shoda, M., & Nagatani, M. (1968). Kinetics of product inhibition in alcohol fermentation. **Biotechnology and Bioengineering**, *10*(6), 845-864. doi:10.1002/bit.260100610
- Andrews, J. F. (1968). A mathematical model for the continuous culture of microorganisms utilizing inhibitory substrates. **Biotechnology and Bioengineering**, *10*(6), 707-723. doi:10.1002/bit.260100602
- Borges, E. R., & Pereira, N., Jr. (2011). Succinic acid production from sugarcane bagasse hemicellulose hydrolysate by *Actinobacillus succinogenes*. **J Ind Microbiol Biotechnol**, *38*(8), 1001-1011. doi:10.1007/s10295-010-0874-7
- Bradfield, M. F., Mohagheghi, A., Salvachua, D., Smith, H., Black, B. A., Dowe, N., Beckham, G. T., & Nicol, W. (2015). Continuous succinic acid production by *Actinobacillus succinogenes* on xylose-enriched hydrolysate. **Biotechnol Biofuels**, *8*, 181. doi:10.1186/s13068-015-0363-3
- Chen, K., Jiang, M., Wei, P., Yao, J., & Wu, H. (2010). Succinic acid production from acid hydrolysate of corn fiber by *Actinobacillus succinogenes*. **Appl Biochem Biotechnol**, *160*(2), 477-485. doi:10.1007/s12010-008-8367-0
- Corona-González, R. I., Bories, A., González-Álvarez, V., & Pelayo-Ortiz, C. (2008). Kinetic study of succinic acid production by *Actinobacillus succinogenes* ZT-130. **Process Biochemistry**, *43*(10), 1047-1053. doi:10.1016/j.procbio.2008.05.011
- Cukalovic, A., & Stevens, C. V. (2008). Feasibility of production methods for succinic acid derivatives: a marriage of renewable resources and chemical technology. **Biofuels, Bioproducts and Biorefining**, *2*(6), 505-529. doi:10.1002/bbb.105

- Dessie, W., Zhang, W., Xin, F., Dong, W., Zhang, M., Ma, J., & Jiang, M. (2018). Succinic acid production from fruit and vegetable wastes hydrolyzed by on-site enzyme mixtures through solid state fermentation. **Bioresource Technology**, 247, 1177-1180. doi:<https://doi.org/10.1016/j.biortech.2017.08.171>
- Edwards, V. H. (1970). The influence of high substrate concentrations on microbial kinetics. **Biotechnology and Bioengineering**, 12(5), 679-712. doi:10.1002/bit.260120504
- Guarnieri, M. T., Chou, Y. C., Salvachua, D., Mohagheghi, A., St John, P. C., Peterson, D. J., Bomble, Y. J., & Beckham, G. T. (2017). Metabolic Engineering of *Actinobacillus succinogenes* Provides Insights into Succinic Acid Biosynthesis. **Appl Environ Microbiol**, 83(17). doi:10.1128/AEM.00996-17
- Han, K., & Levenspiel, O. (1988). Extended monod kinetics for substrate, product, and cell inhibition. **Biotechnol Bioeng**, 32(4), 430-447. doi:10.1002/bit.260320404
- Hasona, A., Kim, Y., Healy, F. G., Ingram, L. O., & Shanmugam, K. T. (2004). Pyruvate formate lyase and acetate kinase are essential for anaerobic growth of *Escherichia coli* on xylose. **J Bacteriol**, 186(22), 7593-7600. doi:10.1128/JB.186.22.7593-7600.2004
- Jantama, K., Haupt, M. J., Svoronos, S. A., Zhang, X., Moore, J. C., Shanmugam, K. T., & Ingram, L. O. (2008a). Combining metabolic engineering and metabolic evolution to develop nonrecombinant strains of *Escherichia coli* C that produce succinate and malate. **Biotechnol Bioeng**, 99(5), 1140-1153. doi:10.1002/bit.21694
- Jantama, K., Zhang, X., Moore, J. C., Shanmugam, K. T., Svoronos, S. A., & Ingram, L. O. (2008b). Eliminating side products and increasing succinate yields in

- engineered strains of *Escherichia coli* C. **Biotechnol Bioeng**, *101*(5), 881-893.
doi:10.1002/bit.22005
- Jiang, M., Liu, S. W., Ma, J. F., Chen, K. Q., Yu, L., Yue, F. F., Xu, B., & Wei, P. (2010). Effect of growth phase feeding strategies on succinate production by metabolically engineered *Escherichia coli*. **Appl Environ Microbiol**, *76*(4), 1298-1300. doi:10.1128/AEM.02190-09
- Jiang, M., Ma, J., Wu, M., Liu, R., Liang, L., Xin, F., Zhang, W., Jia, H., & Dong, W. (2017). Progress of succinic acid production from renewable resources: Metabolic and fermentative strategies. **Bioresour Technol**, *245*(Pt B), 1710-1717. doi:10.1016/j.biortech.2017.05.209
- Khunnonkwao, P., Jantama, S. S., Kanchanatawee, S., & Jantama, K. (2018). Re-engineering *Escherichia coli* KJ122 to enhance the utilization of xylose and xylose/glucose mixture for efficient succinate production in mineral salt medium. **Appl Microbiol Biotechnol**, *102*(1), 127-141. doi:10.1007/s00253-017-8580-2
- Kim, D.-K., Park, J. M., Song, H., & Chang, Y. K. (2016). Kinetic modeling of substrate and product inhibition for 2,3-butanediol production by *Klebsiella oxytoca*. **Biochemical Engineering Journal**, *114*, 94-100. doi:10.1016/j.bej.2016.06.021
- Lee, S. J., Song, H., & Lee, S. Y. (2006). Genome-based metabolic engineering of *Mannheimia succiniciproducens* for succinic acid production. **Appl Environ Microbiol**, *72*(3), 1939-1948. doi:10.1128/AEM.72.3.1939-1948.2006
- Lee, Y.-S., Lee, W. G., Chang, Y. K., & Chang, H. N. (1995). Modelling of ethanol production by *Saccharomyces cerevisiae* from a glucose and maltose mixture.

Biotechnology Letters, 17(8), 791-796. doi:10.1007/BF00129006

Levenspiel, O. (1980). The monod equation: A revisit and a generalization to product inhibition situations. **Biotechnology and Bioengineering**, 22(8), 1671-1687. doi:10.1002/bit.260220810

Li, C., Yang, X., Gao, S., Wang, H., & Lin, C. S. K. (2017). High efficiency succinic acid production from glycerol via *in situ* fibrous bed bioreactor with an engineered *Yarrowia lipolytica*. **Bioresour Technol**, 225, 9-16. Doi:10.106/j.biortech.2016.11.016

Li, Q., Wang, D., Wu, Y., Yang, M., Li, W., Xing, J., & Su, Z. (2010). Kinetic evaluation of products inhibition to succinic acid producers *Escherichia coli* NZN111, AFP111, BL21, and *Actinobacillus succinogenes* 130Z T. **J Microbiol**, 48(3), 290-296. doi:10.1007/s12275-010-9262-2

Li, Y., Li, M., Zhang, X., Yang, P., Liang, Q., & Qi, Q. (2013). A novel whole-phase succinate fermentation strategy with high volumetric productivity in engineered *Escherichia coli*. **Bioresour Technol**, 149, 333-340. doi:10.1016/j.biortech.2013.09.077

Lin, S. K. C., Du, C., Koutinas, A., Wang, R., & Webb, C. (2008). Substrate and product inhibition kinetics in succinic acid production by *Actinobacillus succinogenes*. **Biochemical Engineering Journal**, 41(2), 128-135. doi:10.1016/j.bej.2008.03.013

Litsanov, B., Brocker, M., & Bott, M. (2012). Toward homosuccinate fermentation: metabolic engineering of *Corynebacterium glutamicum* for anaerobic production of succinate from glucose and formate. **Appl Environ Microbiol**, 78(9), 3325-3337. doi:10.1128/AEM.07790-11

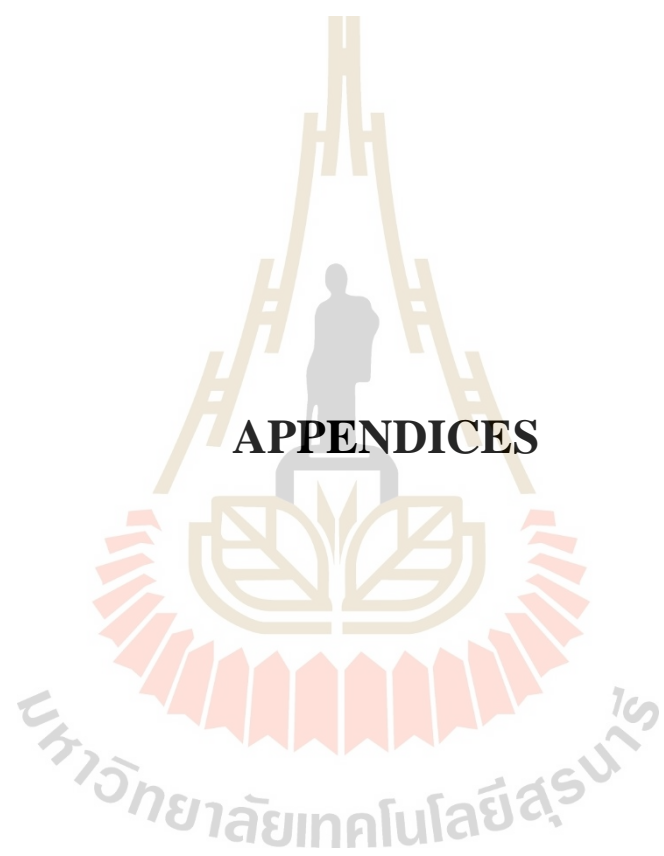
- Luedeking, R., & Piret, E. L. (1959). A kinetic study of the lactic acid fermentation. Batch process at controlled pH. **Journal of Biochemical and Microbiological Technology and Engineering**, *1*(4), 393-412. doi:10.1002/jbmte.390010406
- Luong, J. H. (1987). Generalization of monod kinetics for analysis of growth data with substrate inhibition. **Biotechnol Bioeng**, *29*(2), 242-248. doi:10.1002/bit.260290215
- Luthfi, A. A. I., Jahim, J. M., Harun, S., Tan, J. P., Manaf, S. F. A., & Shah, S. S. M. (2018). Kinetics of the Bioproduction of Succinic Acid by *Actinobacillus succinogenes* from Oil Palm Lignocellulosic Hydrolysate in a Bioreactor. **BioResources**, *13*(4). doi:10.15376/biores.13.4.8279-8294
- McKinlay, J. B., Vieille, C., & Zeikus, J. G. (2007). Prospects for a bio-based succinate industry. **Appl Microbiol Biotechnol**, *76*(4), 727-740. doi:10.1007/s00253-007-1057-y
- Mulchandani, A., Luong, J. H., & Leduy, A. (1988). Batch kinetics of microbial polysaccharide biosynthesis. **Biotechnol Bioeng**, *32*(5), 639-646. doi:10.1002/bit.260320508
- Natarajan, K. A. (2018). Chapter 14 - Experimental and Research Methods in Metals Biotechnology. In K. A. Natarajan (Ed.), *Biotechnology of Metals* (pp. 433-468). Amsterdam: Elsevier.
- Okino, S., Noburyu, R., Suda, M., Jojima, T., Inui, M., & Yukawa, H. (2008). An efficient succinic acid production process in a metabolically engineered *Corynebacterium glutamicum* strain. **Appl Microbiol Biotechnol**, *81*(3), 459-464. doi:10.1007/s00253-008-1668-y
- Pateraki, C., Almqvist, H., Ladakis, D., Lidén, G., Koutinas, A. A., & Vlysidis, A.

- (2016). Modelling succinic acid fermentation using a xylose based substrate. **Biochemical Engineering Journal**, *114*, 26-41. doi:10.1016/j.bej.2016.06.011
- Pinazo, J. M., Domine, M. E., Parvulescu, V., & Petru, F. (2015). Sustainability metrics for succinic acid production: A comparison between biomass-based and petrochemical routes. **Catalysis Today**, *239*, 17-24. doi:10.1016/j.cattod.2014.05.035
- Raab, A. M., Gebhardt, G., Bolotina, N., Weuster-Botz, D., & Lang, C. (2010). Metabolic engineering of *Saccharomyces cerevisiae* for the biotechnological production of succinic acid. **Metab Eng**, *12*(6), 518-525. doi:10.1016/j.ymben.2010.08.005
- Rigaki, A., Webb, C., & Theodoropoulos, C. (2020). Double substrate limitation model for the bio-based production of succinic acid from glycerol. **Biochemical Engineering Journal**, *153*, 107391. doi:https://doi.org/10.1016/j.bej.2019.107391
- Sadhukhan, S., Villa, R., & Sarkar, U. (2016). Microbial production of succinic acid using crude and purified glycerol from a *Crotalaria juncea* based biorefinery. **Biotechnology Reports**, *10*, 84-93. doi:https://doi.org/10.1016/j.btre.2016.03.008
- Salvachua, D., Mohagheghi, A., Smith, H., Bradfield, M. F. A., Nicol, W., Black, B. A., Bidy, M. J., Dowe, N., & Beckham, G. T. (2016). Succinic acid production on xylose-enriched biorefinery streams by *Actinobacillus succinogenes* in batch fermentation. **Biotechnol Biofuels**, *9*, 28. doi:10.1186/s13068-016-0425-1
- Salvachúa, D., Smith, H., St. John, P. C., Mohagheghi, A., Peterson, D. J., Black, B. A., Dowe, N., & Beckham, G. T. (2016). Succinic acid production from

- lignocellulosic hydrolysate by *Basfia succiniciproducens*. **Bioresource Technology**, 214, 558-566. doi:<https://doi.org/10.1016/j.biortech.2016.05.018>
- Sawisit, A., Jantama, K., Zheng, H., Yomano, L. P., York, S. W., Shanmugam, K. T., & Ingram, L. O. (2015). Mutation in galP improved fermentation of mixed sugars to succinate using engineered *Escherichia coli* AS1600a and AM1 mineral salts medium. **Bioresour Technol**, 193, 433-441. doi:10.1016/j.biortech.2015.06.108
- Saxena, R. K., Saran, S., Isar, J., & Kaushik, R. (2017). Production and Applications of Succinic Acid. In *Current Developments in Biotechnology and Bioengineering* (pp. 601-630).
- Song, H., Kim, T. Y., Choi, B. K., Choi, S. J., Nielsen, L. K., Chang, H. N., & Lee, S. Y. (2008). Development of chemically defined medium for *Mannheimia succiniciproducens* based on its genome sequence. **Appl Microbiol Biotechnol**, 79(2), 263-272. doi:10.1007/s00253-008-1425-2
- Song, H., Lee, J. W., Choi, S., You, J. K., Hong, W. H., & Lee, S. Y. (2007). Effects of dissolved CO₂ levels on the growth of *Mannheimia succiniciproducens* and succinic acid production. **Biotechnol Bioeng**, 98(6), 1296-1304. doi:10.1002/bit.21530
- Stanbury, P. F., Whitaker, A., & Hall, S. J. (2017). Chapter 2 - Microbial growth kinetics. In P. F. Stanbury, A. Whitaker, & S. J. Hall (Eds.), *Principles of Fermentation Technology* (Third Edition) (pp. 21-74). Oxford: Butterworth-Heinemann.
- Tampion, J. (1989). *Fermentation kinetics and modelling* C. G. Sinclair & B. Kristiansen (edited by J. D. Bu'Lock), Open University Press, Milton Keynes,

1987. pp. xi + 113, price £14.95. ISBN 0-8448-1509-8. **Journal of Chemical Technology & Biotechnology**, 44(4), 330-330. doi:10.1002/jctb.280440412
- Van Den Heuvel, J. C., & Beftink, H. H. (1988). Kinetic effects of simultaneous inhibition by substrate and product. **Biotechnology and Bioengineering**, 31(7), 718-724. doi:10.1002/bit.260310714
- Varma, A., & Palsson, B. O. (1993). Metabolic Capabilities of *Escherichia coli* II. Optimal Growth Patterns. **Journal of Theoretical Biology**, 165(4), 503-522. doi:https://doi.org/10.1006/jtbi.1993.1203
- Vlysidis, A., Binns, M., Webb, C., & Theodoropoulos, C. (2011). Glycerol utilisation for the production of chemicals: Conversion to succinic acid, a combined experimental and computational study. **Biochemical Engineering Journal**, 58-59, 1-11. doi:10.1016/j.bej.2011.07.004
- Wang, D., Li, Q., Song, Z., Zhou, W., Su, Z., & Xing, J. (2011). High cell density fermentation via a metabolically engineered *Escherichia coli* for the enhanced production of succinic acid. **Journal of Chemical Technology & Biotechnology**, 86(4), 512-518. doi:10.1002/jctb.2543
- Werpy, T., & Petersen, G. (2004). Top Value Added Chemicals from Biomass: Volume I -- Results of Screening for Potential Candidates from Sugars and Synthesis Gas. Retrieved from U.S. Department of Energy:
- Yan, D., Wang, C., Zhou, J., Liu, Y., Yang, M., & Xing, J. (2014). Construction of reductive pathway in *Saccharomyces cerevisiae* for effective succinic acid fermentation at low pH value. **Bioresour Technol**, 156, 232-239. doi:10.1016/j.biortech.2014.01.053
- Yu, J. H., Zhu, L. W., Xia, S. T., Li, H. M., Tang, Y. L., Liang, X. H., Chen, T., &

- Tang, Y. J. (2016). Combinatorial optimization of CO₂ transport and fixation to improve succinate production by promoter engineering. **Biotechnol Bioeng**, *113*(7), 1531-1541. doi:10.1002/bit.25927
- Zhu, L. W., & Tang, Y. J. (2017). Current advances of succinate biosynthesis in metabolically engineered *Escherichia coli*. **Biotechnol Adv**, *35*(8), 1040-1048. doi:10.1016/j.biotechadv.2017.09.007
- Zhu, N., Xia, H., Wang, Z., Zhao, X., & Chen, T. (2013). Engineering of acetate recycling and citrate synthase to improve aerobic succinate production in *Corynebacterium glutamicum*. **PLoS One**, *8*(4), e60659. doi:10.1371/journal.pone.0060659
- Zhu, X., Tan, Z., Xu, H., Chen, J., Tang, J., & Zhang, X. (2014). Metabolic evolution of two reducing equivalent-conserving pathways for high-yield succinate production in *Escherichia coli*. **Metab Eng**, *24*, 87-96. doi:10.1016/j.ymben.2014.05.



APPENDICES

APPENDIX A

THE HPLC STANDARD CURVE

The HPLC standard for analyze substrates and products

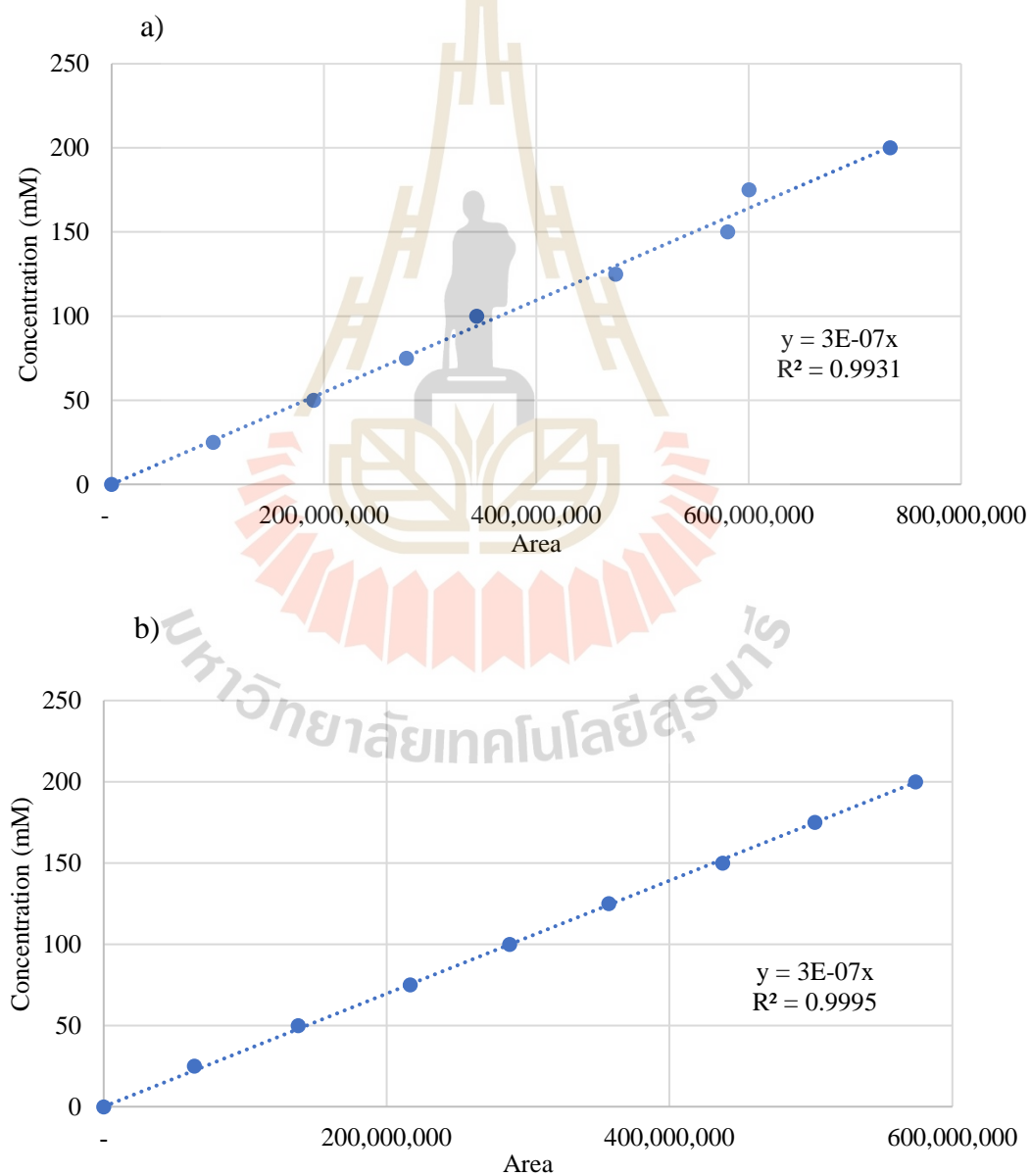


Figure 1A The HPLC standard of (a) glucose and (b) xylose.

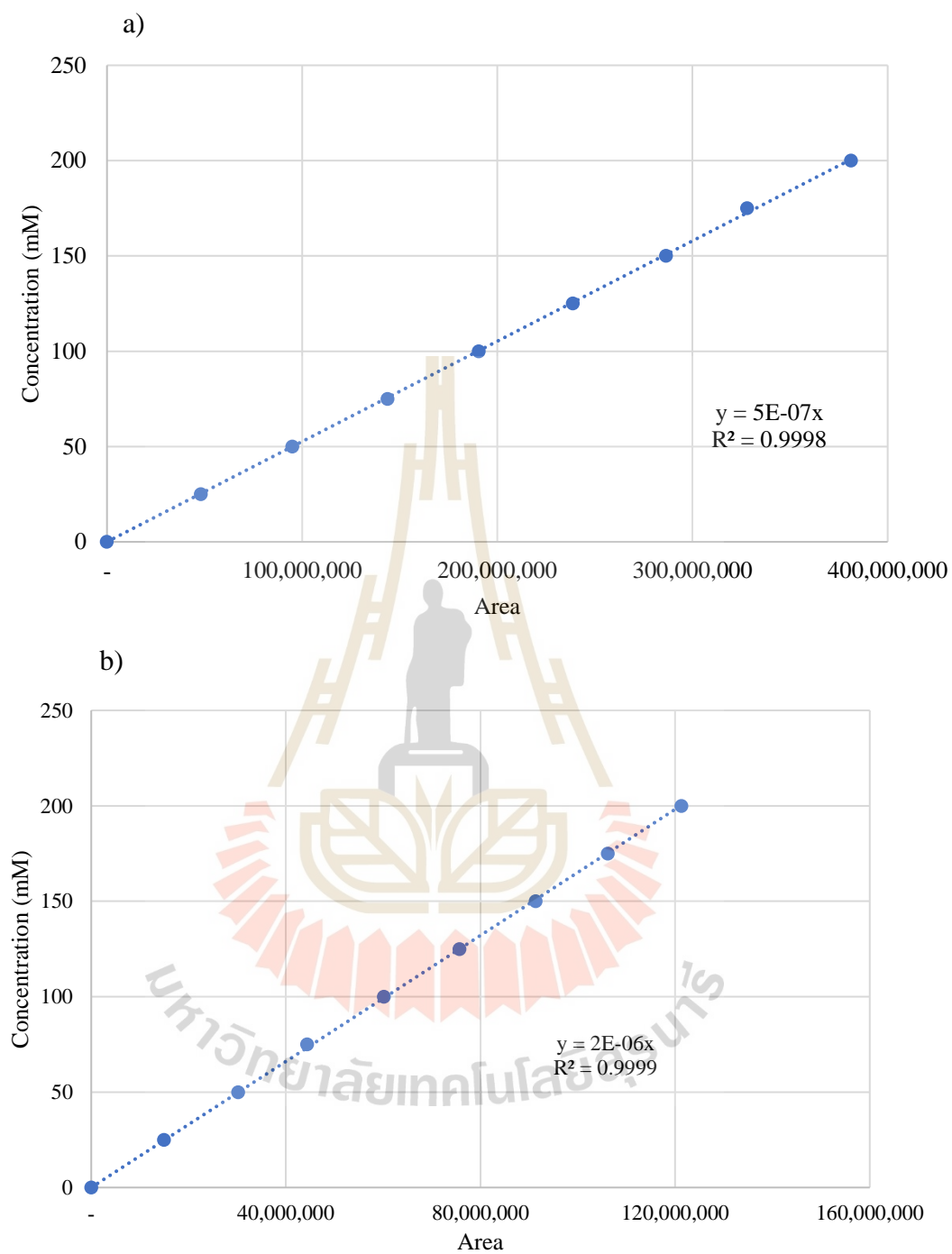


Figure 2A The HPLC standard of (a) succinate and (b) acetate.

APPENDIX B

KINETIC MODEL PARAMETERS

B1. Specific growth rate model

The example of MABLAB script for estimating parameters of the specific growth rate model.

```
Clear
clc
%Import data
load('Cx0_xylose.mat');
load('uexp_xylose.mat');
load('Boundary_condition_growth_xylose.mat');

%Set initial guess
umax = 0.1;
ks = 0.1;
Cxi = 150;
n = 1;

Initial_parameter(1) = umax;
Initial_parameter(2) = ks;
Initial_parameter(3) = Cxi;
Initial_parameter(4) = n;

%Define function
Monod = @(P,Cx0) P(1) .* Cx0 ./ (Cx0 + P(2)) .* (1 - Cx0 ./ P(3)).^P(4);
Growth_Fc = Monod;

%Run parameter estimation
lb = Boundary_condition_growth_xylose(:,1);
ub = Boundary_condition_growth_xylose(:,2);
options = optimoptions ('lsqcurvefit','FiniteDifferenceStepSize',1e-10,'TolFun',1e-10,'TolX',1e-10);
[Predicted_Parameter,renorm,residual,exitflag,output] =
lsqcurvefit(Growth_Fc, Initial_parameter, Cx0_xylose, uexp_xylose, lb, ub,
options);
u_predict = Growth_Fc(Predicted_Parameter,Cx0_xylose);

%Plot experimental data and model prediction
figure('Name','Specific growth rate profiles','NumberTitle','off');
title('The Comparison of experimental and model data')
plot(Cx0_xylose, uexp_xylose,'ro',Cx0_xylose,u_predict,'b-')
xlabel('Initial xylose concentration (g/L)')
ylabel('Specific growth rate (h-1)')
hold off
```

B2. Parameter estimation

The example of MABLAB script for estimating parameters *via* minimization of function $f(pp)$.

```

clear

clc

%Import data
load('Boundary_condition_Xylose.mat');
load('Time_Xylose.mat');
load('Substrate_Xylose.mat');
load('Biomass_Xylose.mat');
load('Succinate_Xylose.mat');
load('Acetate_Xylose.mat');

global row_data column_data Time_exp Biomass_exp Substrate_exp
Succinate_exp Acetate_exp
global umax ks Cxi n

[row_data,column_data] = size(Time_Xylose);
Time_exp = Time_Xylose;
Biomass_exp = Biomass_Xylose;
Substrate_exp = Substrate_Xylose;
Succinate_exp = Succinate_Xylose;
Acetate_exp = Acetate_Xylose;
lb = Boundary_condition_Xylose(:,1);
ub = Boundary_condition_Xylose(:,2);
Fc_estimation = @Fc_Parameter_Estimation_Xylose;

%Set initial guess
umax = 0.495;
ks = 4.94;
Cxi = 143.54;
n = 1.42;
klmax = 0.001;
kl = 1;
Ycx = 0.062;
Ysx = 0.717;
Yax = 0.126;
me = 0.001;
alpha_suc = 1;
beta_suc = 0.01;
alpha_ace = 1;
beta_ace = 0.01;
Csuci = 65.2;
p = 1;

Initial_parameter(1) = klmax;
Initial_parameter(2) = kl;
Initial_parameter(3) = Ycx;
Initial_parameter(4) = Ysx;
Initial_parameter(5) = Yax;
Initial_parameter(6) = me;
Initial_parameter(7) = alpha_suc;
Initial_parameter(8) = beta_suc;
Initial_parameter(9) = alpha_ace;
Initial_parameter(10) = beta_ace;

```

```

Initial_parameter(11) = Csuci;
Initial_parameter(12) = p;

%Run parameter estimation
A = [];
b = [];
Aeq = [];
beq = [];
nonlcon = [];options = optimset('PlotFcns', { @optimplotx
@optimplotfunccount @optimplotfval @optimplotconstrviolation });
[Predicted_Parameter,fval,exitflag,output] =
fmincon(Fc_estimation,Initial_parameter,A,b,Aeq,beq,lb,ub,nonlcon,options);
Predicted_Parameter = Predicted_Parameter';
Initial_parameter = Initial_parameter';
[Total_min, Data_set, Time_pred, Biomass_pred, Substrate_pred,
Succinate_pred, Acetate_pred] = Fc_estimation(Predicted_Parameter);

%Plot graph experimental data and model prediction
figure
for i = 1:1:column_data
subplot(2,2,i)
hold on
yyaxis left
title(sprintf('Kinetic Equation\n\t\tThe initial substrate concentration =
%.3f',Substrate_Xylose(1,i)))
plot(Time_Xylose(1:Data_set(i),i),
Substrate_Xylose(1:Data_set(i),i),'ro',Time_Xylose(1:Data_set(i),i),Succinat
e_Xylose(1:Data_set(i),i),'bo',Time_Xylose(1:Data_set(i),i),Acetate_Xylose(1
:Data_set(i),i),'mo')
plot(Time_pred(1:Data_set(i),i), Substrate_pred(1:Data_set(i),i),'r-
',Time_pred(1:Data_set(i),i),Succinate_pred(1:Data_set(i),i),'b-
',Time_pred(1:Data_set(i),i),Acetate_pred(1:Data_set(i),i),'m-')
xlabel('Time (h)')
ylabel('Concentration (g/L)')
yyaxis right
plot(Time_Xylose(1:Data_set(i),i), Biomass_Xylose(1:Data_set(i),i),'go')
plot(Time_pred(1:Data_set(i),i), Biomass_pred(1:Data_set(i),i),'g-')
ylabel('Biomass concentration (g/L)')
hold off
end

```

The example of MABLAB function for estimating parameters via minimization of function $f(pp)$.

```
function [Total_min, Data_set, Time_pred, Biomass_pred, Substrate_pred,
Succinate_pred, Acetate_pred] =
Fc_Parameter_Estimation_Xylose(Initial_parameter)

global row_data column_data Time_exp Biomass_exp Substrate_exp Succinate_exp
Acetate_exp
global umax ks Cxi n

Data_set      = zeros(column_data);
Time_pred     = zeros(row_data,column_data);
Biomass_pred  = zeros(row_data,column_data);
Substrate_pred = zeros(row_data,column_data);
Succinate_pred = zeros(row_data,column_data);
Acetate_pred  = zeros(row_data,column_data);

function Diff_Y = Dif_Eq(t,V)

    klmax      = Initial_parameter(1);
    kl         = Initial_parameter(2);
    Ycx        = Initial_parameter(3);
    Ysx        = Initial_parameter(4);
    Yax        = Initial_parameter(5);
    me         = Initial_parameter(6);
    alpha_suc  = Initial_parameter(7);
    beta_suc   = Initial_parameter(8);
    alpha_ace  = Initial_parameter(9);
    beta_ace   = Initial_parameter(10);
    Csuci      = Initial_parameter(11);
    p          = Initial_parameter(12);

    u = umax .* V(2) ./ (V(2) + ks) .* ((1 - (V(2) ./ Cxi)) .^ n) .*
        ((1 - (V(3) ./ Csuci)) .^ p);
    d = klmax .* kl ./ (V(2) + kl);
    Diff_Y(1) = (u - d) .* V(1);
    delta = 1 ./ Ycx + alpha_suc ./ Ysx + alpha_ace ./ Yax;
    gamma = beta_suc ./ Ysx + beta_ace ./ Yax + me;
    Diff_Y(2) = -1 .* (delta .* (u - d) .* V(1) + gamma .* V(1));
    Diff_Y(3) = alpha_suc .* (u - d) .* V(1) + beta_suc .* V(1);
    Diff_Y(4) = alpha_ace .* (u - d) .* V(1) + beta_ace .* V(1);
    Diff_Y = Diff_Y';

end

for column_estimate = 1:1:column_data
    Row_datanew = 0;
    for Row_estimate = 1:1:row_data

        if Substrate_exp(Row_estimate,column_estimate) == 0
            break ;
        else
            Row_datanew = Row_datanew + 1;
        end
    end

    Time_exp_new(1:Row_datanew,1) =
    Time_exp(1:Row_datanew,column_estimate);
```

```

    Biomass_exp_new(1:Row_datanew,1) =
    Biomass_exp(1:Row_datanew,column_estimate);
    Substrat_exp_enuw(1:Row_datanew,1) =
    Substrate_exp(1:Row_datanew,column_estimate);
    Succinate_exp_new(1:Row_datanew,1) =
    Succinate_exp(1:Row_datanew,column_estimate);
    Acetate_exp_new(1:Row_datanew,1) =
    Acetate_exp(1:Row_datanew,column_estimate);

    Time_span = Time_exp_new;
    V0 = [Biomass_exp_new(1,1), Substrat_exp_enuw(1,1),
    Succinate_exp_new(1,1), Acetate_exp_new(1,1)];
    [t, Diffvalue] = ode23s(@Dif_Eq, Time_span, V0);

    [row_pred,~] = size(t);

    Time_pred(1:row_pred,column_estimate) = t;
    Biomass_pred(1:row_pred,column_estimate) = Diffvalue(:,1);
    Substrate_pred(1:row_pred,column_estimate) = Diffvalue(:,2);
    Succinate_pred(1:row_pred,column_estimate) = Diffvalue(:,3);
    Acetate_pred(1:row_pred,column_estimate) = Diffvalue(:,4);

    Data_set(column_estimate) = Row_datanew;
    clear Time_exp_new;
    clear Biomass_exp_new;
    clear Substrat_exp_enuw;
    clear Succinate_exp_new;
    clear Acetate_exp_new;

end

Total_min = 0;
for data = 1:1:column_data
    min_sum_biomass = sum(((Biomass_exp(1:Data_set(data),data)-
    Biomass_pred(1:Data_set(data),data))/Biomass_exp(1:Data_set(data),data)).^2)
    ;
    min_sum_substrate = sum(((Substrate_exp(1:Data_set(data),data)-
    Substrate_pred(1:Data_set(data),data))/Substrate_exp(1:Data_set(data),data))
    .^2);
    min_sum_succinate = sum(((Succinate_exp(1:Data_set(data),data)-
    Succinate_pred(1:Data_set(data),data))/Succinate_exp(1:Data_set(data),data))
    .^2);
    min_sum_acetate = sum(((Acetate_exp(1:Data_set(data),data)-
    Acetate_pred(1:Data_set(data),data))/Acetate_exp(1:Data_set(data),data)).^2)
    ;

    min_sum_experimant = min_sum_biomass + min_sum_substrate + min_sum_succinate
    + min_sum_acetate;
    Total_min = sum(min_sum_experimant);
    Total_min = Total_min + Total_min;
end

end

```

B3. Parametric sensitivity

The example of MABLAB script for analyzing parametric sensitivity.

```

clear

clc

load('Time_Xylose.mat');
load('Biomass_Xylose.mat');
load('Substrate_Xylose.mat');
load('Succinate_Xylose.mat');
load('Acetate_Xylose.mat');

global row_data column_data Time_exp Biomass_exp Substrate_exp
Succinate_exp Acetate_exp

Time_exp = Time_Xylose;
Biomass_exp = Biomass_Xylose;
Substrate_exp = Substrate_Xylose;
Succinate_exp = Succinate_Xylose;
Acetate_exp = Acetate_Xylose;

[row_data,column_data] = size(Time_Xylose);

umax      = 0.495;
ks        = 4.94;
Cxi       = 143.54;
n         = 1.421;
klmax     = 0.36;
kl        = 9.42;
Ycx       = 0.721;
Ysx       = 0.960;
Yax       = 0.879;
me        = 0.005;
alpha_suc = 2.222;
beta_suc  = 0.864;
alpha_ace = 1.008;
beta_ace  = 0.139;
Csuci     = 68.19;
p         = 2.27;

Original_point(1) = umax;
Original_point(2) = ks;
Original_point(3) = Cxi;
Original_point(4) = n;
Original_point(5) = klmax;
Original_point(6) = kl;
Original_point(7) = Ycx;
Original_point(8) = Ysx;
Original_point(9) = Yax;
Original_point(10) = me;
Original_point(11) = alpha_suc;
Original_point(12) = beta_suc;
Original_point(13) = alpha_ace;
Original_point(14) = beta_ace;
Original_point(15) = Csuci;
Original_point(16) = p;

No_parameter = 16;

```

```

Percent_change = 5;
Min_RMSE = zeros(5,No_parameter);
Percent_change_ObjFc = zeros(5,No_parameter);
Reset_point = Original_point;
Sensitivity_Fc = @Fc_Sensitivity_analysis_Xylose_model;

Max_value = Original_point + (Percent_change./100) .* Original_point;
Min_value = Original_point - (Percent_change./100) .* Original_point;

Point_Interval = zeros(5,No_parameter);
Percent_change_Parameter = zeros(5,1);
Parameter_Name = [ "umax" "ks" "Cxi" "n" "klmax" "kl" "Ycx" "Ysx" "Yax" "me"
"alpha_suc" "beta_suc" "alpha_ace" "beta_ace" "Csuci" "p"];

for p = 1:1:No_parameter
Point_Interval(1:3,p) = linspace(Max_value(p),Original_point(p),3);
Point_Interval(3:5,p) = linspace(Original_point(p),Min_value(p),3);

figure('Name','Sensitivity analysis','NumberTitle','off');
title(sprintf('The %%Change of the output value versus %%Change of
%s',Parameter_Name(p)))
ylabel('%%Change of the output value')
xlabel(sprintf('%%Change of %s',Parameter_Name(p)))
hold on

for i = 1:1:Percent_change
Percent_change_Parameter(i,p) = (Point_Interval(i,p) -
Original_point(p))/Original_point(p)*100;
Original_point(1,p) = Point_Interval(i,p);
[Total_min] = Sensitivity_Fc(Original_point);
Min_RMSE(i,p) = Total_min;
Original_point = Reset_point;
end
Percent_change_ObjFc(:,p) = (Min_RMSE(:,p) -
Min_RMSE(5,p))/Min_RMSE(5,p)*100;
grid on
plot(Percent_change_Parameter(:,p),Percent_change_ObjFc(:,p),'go-');
hold off
end

```

BIOGRAPHY

Mr. Tassanon Chaleewong was born in Khon Kaen on April 4, 1996. He received a Bachelor of Engineering in Chemical engineering (First class honor) in 2018 from Suranaree University of Technology, Nakhon Ratchasima, Thailand. After graduation, he decided to study the master program in the field of Biotechnology at school of Biotechnology, Institute of Agricultural Technology, Suranaree University of Technology, Nakhon Ratchasima, Thailand.

